JOURNAL OF CHEMICAL INFORMATION AND MODELING

Article

pubs.acs.org/jcim

Molecular Dynamics Simulations and Structural Network Analysis of c-Abl and c-Src Kinase Core Proteins: Capturing Allosteric Mechanisms and Communication Pathways from Residue Centrality

Amanda Tse[†] and Gennady M. Verkhivker*[,†,‡]

[†]Graduate Program in Computational and Data Sciences, Department of Computational Sciences, Schmid College of Science and Technology, Chapman University, One University Drive, Orange, California 92866, United States

[‡]Chapman University School of Pharmacy, Irvine, California 92618, United States

Supporting Information

ABSTRACT: The Abl and Src tyrosine kinases play a fundamental regulatory role in orchestrating functional processes in cellular networks and represent an important class of therapeutic targets. Crystallographic studies of these kinases have revealed a similar structural organization of multidomain complexes that confers salient features of their regulatory mechanisms. Molecular characterization of the interaction networks and regulatory residues by which the SH3 and SH2 domains act cooperatively with the catalytic domain to suppress or promote kinase activation presents an active area of structural, biochemical, and computational investigations. In this work, we combine biophysical simulations with computational modeling of the residue interaction networks to characterize allosteric mechanisms of kinase regulation and gain insight into differential sensitivity of c-Abl and c-Src kinases to specific drug binding. Using these approaches, we examine dynamics of cooperative rearrangements in the residue interaction networks and elucidate the structural role of regulatory residues responsible for modulation of kinase activity. We have found that global network parameters such as residue centrality can unambiguously distinguish functional sites that are responsible for mediating allosteric interactions in the regulatory assemblies. This study has revealed mechanistic aspects of allosteric mechanisms and communication pathways by which the SH3 and SH2 domains may exert their regulatory influence on the catalytic domain and kinase activity. We have also found that high centrality residues can be linked to each other to form efficient and robust routes that transmit allosteric signals between spatially separated regulatory regions. The presented results have demonstrated that global features of the residue interaction networks may serve as transparent and robust indicators of kinase regulatory mechanisms and accurately pinpoint key functional residues.

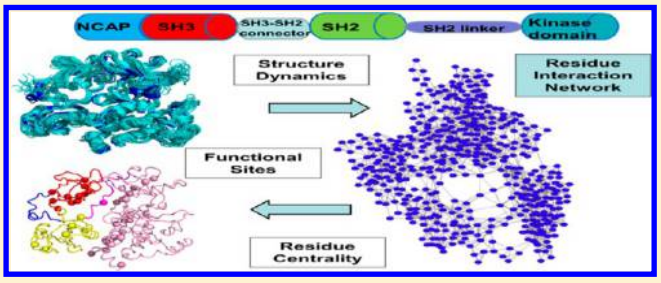

INTRODUCTION

Protein kinase genes are signaling switches that direct functional processes and protein communications in cellular networks and signal transduction pathways.[1,2] The human protein kinases, that represent one of the largest protein families, are regulated by different mechanisms including phosphorylation of the activation loops, autoinhibition, and allosteric activation by protein binding partners that enable the kinase domain (KD) to adopt a catalytically competent conformation and attain activity.[3−11] The Abelson (Abl) family of nonreceptor protein tyrosine kinases consists of two members, c-Abl and the Abl-related gene (Arg), that are involved in interactions with a multitude of cellular proteins, linking extracellular stimuli to signaling pathways that control cell growth, survival, invasion, adhesion and migration.[12−14] Each Abl protein contains an SH3-SH2-KD (Src homology 3-Src homology 2-kinase domain) domain cassette, which confers autoregulated kinase activity and is common among non-receptor tyrosine kinases.[12−14] The Src family of cytoplasmic nonreceptor protein tyrosine kinases (c-Src, Lck, Fgr, Fyn, c-Yes, Blk, Hck, and Lyn kinases) can integrate diverse cellular signals and are involved in mediating Abl kinase activity and signal transduction.[15−17] Structural and biochemical studies have revealed autoinhibitory mechanisms that can modulate and constrain catalytic activity and substrate specificity of the c-Abl and c-Src kinases. These kinases share the same SH3-SH2-KD modular organization that confers salient features of their regulatory mechanisms. Crystallographic studies have provided a molecular framework of activation mechanisms by detailing a common structural organization of the regulatory complexes for the c-Src[18−20] and c-Abl kinases.[21−24] In the autoinhibitory complexes, the SH3 domain binds to the linker that connects the SH2 domain and the KD, while the SH2 domain interacts with the C-terminal lobe of the KD playing a negative regulatory role as an intramolecular autoinhibitory "clamp" that maintains the KD in a conformation with low catalytic activity (Figure 1). The disengagement of the SH3-SH2 domains

Received: April 27, 2015
Published: August 3, 2015

DOI: 10.1021/acs.jcim.5b00240
J. Chem. Inf. Model. 2015, 55, 1645−1662

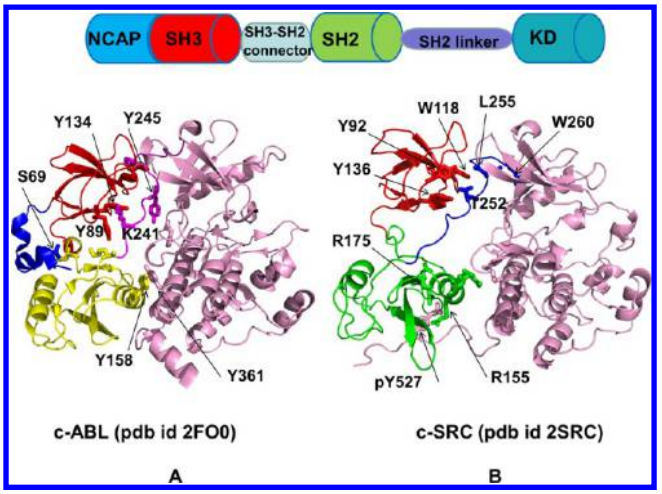

Figure 1. Structural organization of the c-Abl and c-Src regulatory complexes. Common domain organization of the c-Abl and c-Src kinases is schematically shown at the top. The core domains in c-Abl are NCap, N-terminal region; SH3, Src homology domain 3; SH2, Src homology domain 2; SH2 Linker, SH2-kinase linker; and KD, kinase domain. (A) Crystal structure of the downregulated c-Abl complex (pdb id 2FO0) rendered in ribbons and colored by domains: NCap (blue), SH3 (red), SH2 (green), SH2 linker (magenta), and KD (pink). (B) Crystal structure of the autoinhibitory c-Src complex (pdb id 2SRC) shown in ribbons and colored by domains: SH3 (red), SH2 (green), SH2 linker (magenta), and KD (pink). The functional regulatory residues and phosphorylation tyrosine sites are annotated and shown in colored bold sticks.

relieves the autoinhibitory constraints in c-Src and c-Abl kinases and yields an activated form. Small-angle X-ray scattering (SAXS) reconstruction of an activated form of c-Abl protein in solution has confirmed that upon kinase activation the SH2 and SH3 domains switch from a compact assembly to an elongated arrangement. The active c-Abl structure yielded a fully extended conformation with the KD, SH2, and SH3 domains in a linear arrangement, yet the position of the SH3 domain could not be determined.[22]

Recent structural and biochemical investigations of c-Abl kinase[25−27] have reported molecular details of the regulatory interactions by which the SH3 and SH2 domains can suppress or promote kinase activation. The SH3 domain of c-Abl plays a major role in stabilizing the autoinhibitory state (Figure 1A) by interacting with the N-terminal lobe of KD and the SH2-kinase linker. Biophysical studies have demonstrated that the SH3 domain can sustain its interactions with the Abl linker even in the absence of the KD,[28,29] indicating that robustness of these autoinhibitory interactions may be dictated by their central role in kinase regulation. Furthermore, the enhanced SH3-linker interactions, induced by mutations of the linker prolines, could allosterically strengthen the autoinhibitory constraints and suppress the kinase activity, rendering the improved c-Abl sensitivity to small molecule inhibitors.[30] Conversely, mutations or deletions in the SH3 domain and the SH2-kinase linker can trigger the release of autoinhibitory constraints, leading to the enhanced activation potential of c-Abl. The crystal structure of a downregulated c-Abl core protein is composed of a myristoylated (Myr) N-terminal "cap" (NCap) followed by the SH3, SH2, and kinase domains (Figure 1A). In this structure, the NCap fragment can form direct interactions with the SH2 domain and the SH3−SH2 connector, strengthening the autoinhibitory "grip" over the catalytic core.[31]

The disruption of key autoinhibitory interactions by phosphorylation of tyrosine residues is crucial for positive regulation of Abl activity.[32−34] Biochemical studies have demonstrated that phosphorylation of the SH3 residues Y89 and Y134 can interfere with the SH3-linker binding (Figure 1A), thereby disrupting key negative regulatory interactions and leading to kinase activation.[34,35] Phosphorylation of Y245 in the linker can also disrupt the SH3-linker interactions and promote Abl kinase activity.[35,36] At the same time, mutation of Y245 that prevents its phosphorylation can reduce maximal activation of c-Abl by ∼50% in vitro.[33] Similarly, mutations of Y158 in the SH2-KD interface have shown an increase in kinase activity,[13] suggesting that stabilizing SH2 interactions with the C-lobe of the catalytic core may be required for downregulation of kinase activity. The Src family kinases such as Hck, Lyn, and Fyn can phosphorylate Y89 in the SH3 domain of Abl (Figure 1B) and exert control over Abl kinase activity by perturbing the autoinhibitory SH3-linker interactions.[36,37] These studies have shown that phosphorylation and single mutations of functional residues can perturb networks of autoinhibitory interactions and induce large conformational rearrangements between the inactive and active kinase states.

Crystallographic studies of the isolated catalytic domains have revealed that activity of c-Abl and c-Src kinases may be also supported through conformational changes in the key functional regions of the catalytic core: the glycine rich P-loop, the Asp-Phe-Gly (DFG) motif, the regulatory αC-helix, and the activation loop (A-loop).[38−41] A particularly important control element of kinase regulation is the A-loop that can leverage both conformational and phosphorylation preferences to modulate kinase activity and determine substrate access. The C-lobe of the catalytic core contributes to the active site through the A-loop with a single tyrosine site (Y412) that undergoes autophosphorylation by other tyrosine kinases.[25,26] Structural and functional analyses have indicated that the isolated Abl KD has an intrinsically closed DFG-out conformation, where Y412 acts as a pseudosubstrate not accessible for phosphorylation. Phosphorylation of Y412 in the A-loop can stabilize an active kinase conformation and is coupled with the increased catalytic activity of c-Abl.[33,42] Biochemical studies have also discovered that an intramolecular SH2-KD interaction in Abl can be both necessary and sufficient for high catalytic activity of the enzyme, confirming a positive regulatory role of this interaction in kinase function.[43] A recent "tour de force" investigation of Abl regulation[44] has unveiled that the SH2-KD interactions can allosterically induce kinase activation by converting the KD from an intrinsically inactive conformation to an active form, which is then stabilized via phosphorylation of Y412 in the A-loop. The most recent work from the Kuriyan lab has presented a new crystal structure of an SH2-KD construct, revealing that the SH2-KD interactions in the active complex can promote processive phosphorylation and moderately enhance kinase activity.[45] NMR and SAXS studies of the modified c-Abl core protein lacking the myristoylated NCap has shown that the apo c-Abl form can adopt a "closed" conformation, which is similar to the down-regulated Abl core crystal structure.[46] Surprisingly, the presence of Imatinib could lead to an "open" conformation, where the SH3 and SH2 domains are displaced from the back of the KD. Remarkably, the combination of Imatinib with the allosteric inhibitor GNF-5 can restore the closed, inactivated state. These structural studies of c-Abl complexes with inhibitors have also established that the SH2 and SH3 domains can adopt a range of

DOI: 10.1021/acs.jcim.5b00240
J. Chem. Inf. Model. 2015, 55, 1645−1662

different positions with respect to KD, confirming that the SH3-linker interactions may be sufficient to maintain c-Abl in a down-regulated conformation.[46]

The discovery of Imatinib, a highly selective inhibitor that targets the inactive, downregulated form of c-Abl, has marked a historical breakthrough in the development of the tyrosine kinase inhibitors combating chronic myeloid leukemia (CML).[38,39] A large number of Imatinib-resistant Abl mutants emerging at the advanced disease stages are associated not only with the binding site and catalytic domain residues[47] but could also arise in the SH3 and SH2 domains, the SH2 linker, and SH3-SH2 connectors.[48] While Imatinib is a potent inhibitor of c-Abl, it does not inhibit c-Src even though Imatinib has been crystallized with c-Abl and c-Src in virtually identical inactive conformations.[49] The high c-Abl selectivity for Imatinib over closely related c-Src kinase was proposed to result from the higher energetic price for adopting Imatinib-bound conformation by c-Src. However, this mechanism was challenged in a subsequent study, where a series of inhibitors derived from the Imatinib scaffold appeared to bind with equally high potency to both c-Src and c-Abl kinase domains, while adopting similar inactive DFG-out conformation in the crystal structures.[50] Computational studies have characterized free energy landscapes in c-Abl and c-Src kinases and showed that the stability difference between the DFG-out and DFG-in conformations of c-Src may be larger than in c-Abl, and conformational selection may underlie the mechanism of Imatinib specificity.[51,52] Molecular dynamics (MD) simulations and free energy calculations combined with isothermal titration calorimetry have quantified energetics of conformational transitions in c-Abl and c-Src kinases,[53] confirming that a more favorable kinetic accessibility and thermodynamic stability of the DFG-out conformation in c-Abl may determine Imatinib selectivity. Subsequent investigations using absolute free energy computations have reconciled computational and experimental data by showing that Imatinib binding specificity may be controlled by a cumulative effect of conformational selection, favoring stabilization of the inactive c-Abl conformation, and broadly distributed variations in the inhibitor-kinase interactions.[54] MD simulations and free energy simulations of Imatinib binding to inactive structures of c-Abl, c-Kit, Lck, and c-Src kinase domains indicated a crucial role of van der Waals dispersive interactions in determining binding specificity with c-Abl.[55,56] Recently, a systematic analysis of inhibitors that stabilize an Imatinib-like inactive conformation have revealed that ligands that are equipotent against Abl and Src showed a small difference in inhibition between unphosphorylated and phosphorylated A-loop forms, while inhibitors that selective for c-Abl over c-Src were sensitive to the phosphorylation state of the A-loop in c-Abl.[57] Hence, the high selectivity and strong sensitivity of Imatinib toward the unphosphorylated form of c-Abl is not a universal characteristic of kinase inhibitors that stabilize the DFG-out conformation. It was suggested that allosteric coupling between the P-loop and A-loop regions could modulate differences in thermodynamic stability of c-Abl and c-Src kinase conformations, thus fine-tuning binding preferences of specific inhibitors. Steady-state fluorescence kinetics and NMR spectroscopy have studied directly the process of Imatinib binding to the catalytic domain of Abl and Src with millisecond time resolution,[58] suggesting that the energy landscape of Abl kinase may combine conformational selection with an induced fit to enable specific Imatinib binding. These experiments have also revealed that Imatinib binding may cause chemical-shift perturbations distributed over a large fraction of the protein structure, advocating for a global conformational change that was also seen in the NMR study of full-length Abl.[46]

Computational approaches have studied the atomic details of the protein kinase dynamics and regulation at different levels of complexity: from detailed analyses of the catalytic domain and drug resistance[51−59] to simulations of the regulatory assemblies.[60−64] In our previous studies, we analyzed mechanisms of allosteric kinase regulation by integrating multiscale simulations and modeling of long-range communications.[60,61] A multidisciplinary approach combining simulations, functional assays, and mutagenesis has characterized the interdomain coupling in the active Abl complex, suggesting that the SH2-KD interactions can allosterically stabilize the catalytically competent position of the αC-helix and thus exert control over kinase activity.[62] Microsecond all-atom simulations and differential scanning calorimetry have investigated the dynamics of the SH3-SH2 tandem that operates as a two-state switch, alternating between conformations observed in the autoinhibited and active complexes.[63] The biophysical, biochemical, and computational studies of Abl and Src regulation have indicated a complex interplay between the SH3 and SH2 domains, the SH2 linker, and the catalytic domain. Although substantial progress has been made in understanding the structural basis of kinase regulation and drug sensitivity, molecular details underlying the interdomain allosteric communications in the c-Abl and c-Src complexes are yet to be fully understood.

Functional significance of conformational states can be described through global rearrangements in the residue interaction networks that contribute to large conformational changes. These networks are often controlled by critical functional residues that determine relative conformational populations and allosteric communications in the inactive and active kinase states.[64,65] A graph-based representation of protein structures yields a convenient description of residue interaction networks,[66−69] providing a robust framework for understanding allosteric communications in protein systems. Topology-based network parameters describing node centrality (degree, closeness, and betweenness) have been exploited to predict protein−protein interactions,[70,71] protein−DNA interfaces,[72] ligand binding sites,[73,74] and catalytic residues in enzymes.[75] These studies have linked organization of protein structure networks with structural stability and high connectivity of functional residues, particularly indicating that residues involved in short path length communications could mediate signaling.[76] Graph-based protein networks that incorporated topology-based residue connectivity and contact maps of residues cross-correlations obtained from MD simulations[77,78] have provided important insights into structural mechanisms underlying allosteric interactions and communication pathways in various protein systems.[79−85] By using connectivity networks of interacting residues, computational approaches have characterized rigid and flexible regions in protein structures, explaining thermal stability and activity of various proteins.[86−88]

In this work, we present a multifaceted network-based analysis integrated with biophysical simulations to model allosteric mechanisms of kinase regulation and characterize molecular interactions underlying differential sensitivity of c-Abl and c-Src kinases to specific drug binding. MD simulations of the catalytic core and regulatory complexes in c-Abl and c-

DOI: 10.1021/acs.jcim.5b00240
J. Chem. Inf. Model. 2015, 55, 1645−1662

Src kinases are combined with the structure-based network modeling to determine organization of the residue interaction networks and allosteric communication pathways across all functional states. By using global network parameters such as residue centrality we determine cooperative rearrangements in the residue interaction networks and identify global mediating sites that coordinate kinase activity. This study reveals that residue-based centrality can unambiguously distinguish functional sites responsible for regulatory interactions in the autoinhibitory and active complexes. Modeling of the residue interaction networks is leveraged in reconstruction of communication pathways in the kinase assemblies, providing a plausible mechanistic view of allosteric mechanisms by which the SH3 and SH2 domains may exert their regulatory influence on kinase activity. The structure-based network approach provides a simple and transparent view of structural stability and function, showing how the efficiency and robustness of the allosteric interaction networks in c-Abl and c-Src kinases may be linked with their binding preferences and selectivity profiles.

MATERIALS AND METHODS

MD Simulations and Analysis of Collective Motions. MD simulations of the c-Abl and c-Src kinase crystal structures (500 ns for each structure) were performed for different forms of the catalytic domain and for the regulatory complexes. The crystal structures of the c-Abl and c-Src kinases were obtained from the Protein Data Bank.[89] A spectrum of simulated KD crystal structures included the inactive conformations (pdb id 1IEP, 1OPJ for c-Abl, and 2OIQ for c-Src), the Cdk/Src-like inactive forms (pdb id 2G1T for c-Abl and 2SRC for c-Src), and the active conformations (pdb id 2GQG for c-Abl and 3G5D for c-Src). The simulated crystal structures of the regulatory complexes included the autoinhibitory complexes pdb id 2FO0 for c-Abl and 2SRC for c-Src) and active complexes (pdb id 1OPL chain B for c-Abl and 1Y57 for c-Src). The retrieved structures were examined for missing and disordered segments. The missing residues, unresolved structural segments, and disordered loops were modeled with the ArchPRED server.[90]

MD simulations were carried out using NAMD 2.6 package[91] with the CHARMM27 force field[92] and the explicit TIP3P water model. The employed MD protocol is consistent with the overall setup that was described in details in our earlier studies.[93] An NPT production simulation was run on the equilibrated structures for 500 ns keeping the temperature at 300 K and constant pressure (1 atm) using Langevin piston coupling algorithm. Principal component analysis (PCA) of the MD conformational ensembles was performed using the CARMA package.[94] The frames were saved every 5 ps, and a total of 10 000 frames were used to compute the correlation matrices for each simulation.

Local Structural Parameters: Relative Solvent Accessibility and Residue Depth. We have computed the relative solvent accessibility parameter (RSA) that is defined as the ratio of the absolute solvent accessible surface area (SASA) of that residue observed in a given structure and the maximum attainable value of the solvent-exposed surface area for this residue.[95] According to this model, residues are considered to be solvent exposed if the ratio value exceeds 50% and to be buried if the ratio is less than 20%. Analytical SASA is estimated computationally using analytical equations and their first and second derivatives and was computed using web server GetArea.[95] Residue depth measures the closest distance of the residue to bulk solvent.[96] In the first step, the protein molecule is solvated and water molecules that clash with atoms of the protein are removed from the box. Solvent dynamics is mimicked by repeated solvation each time in a different orientation. At each iteration, the value of a residue depth is computed as the distance from a residue to the closest molecule of bulk water. The reported parameter is the average depth over all solvation iterations. The total number of applied solvation cycles was 100. Both parameters are known to correlate with the effects of mutations on protein stability and protein interactions.

Protein Structure Network Construction. In the protein structure network analysis, a graph-based representation of proteins was used in which amino acid residues were considered as nodes connected by edges corresponding to the nonbonding residue−residue interactions. The details of the construction of such a graph at a particular interaction cutoff (I_{min}) were extensively discussed.[77,78] Here, we describe the main steps in the construction of protein structure networks adopted in our study. The interactions between side chain atoms of amino acid residues (nodes) define edges of the protein structure network and are evaluated from the normalized number of contacts between nodes. The noncovalent interactions between sequence neighbors are ignored in the graph construction. The interaction between two residues i and j is measured as

$$I_{ij} = \frac{n_{ij}}{\sqrt{(N_i \times N_j)}} \times 100 \quad (1)$$

In the original formulation of the graph construction procedure,[77,78] the interaction parameter was also defined as a percentage given by

$$I_{ij} = \frac{n_{ij}}{\sqrt{(N_i \times N_j)}} \times 100 \quad (2)$$

where n_{ij} is number of distinct atom pairs between the side chains of amino acid residues i and j that lie within a distance of 4.5 Å. N_i and N_j are the normalization factors for residues i and j respectively. We have determined the normalization factors N_i for all 20 residue types as was described in previous studies.[77] The number of interaction pairs including main-chain and side-chain made by residue type i with all its surrounding residues is also evaluated. The normalization factors take into account the differences in the sizes of the side chains of the different residue types and their propensity to make the maximum number of contacts with other amino acid residues in protein structures. The pair of residues with the interaction I_{ij} greater than a user-defined cutoff (I_{min}) are connected by edges and produce a protein structure network graph for a given interaction cutoff I_{min}. According to the analysis of a large number of protein structures, I_{min} values could vary from 1% to 15%, where the lower I_{min}, the higher is the graph connectivity. The optimal interaction cutoff, that can produce adequate graph representations for a wide range of protein structures, was determined as the transition point for the largest connected cluster.[77] According to this definition, the I_{min} value often lies in the range 2−4% for a diverse spectrum of protein systems and molecular complexes.[77−82] A similar analysis was conducted in our study. In the graph-based analysis of the protein kinase structures performed in the present study, at I_{min} = 1%, all residue nodes are connected by edges, while at I_{min} = 10%, there are typically very few residue nodes connected by

DOI: 10.1021/acs.jcim.5b00240
J. Chem. Inf. Model. 2015, 55, 1645−1662

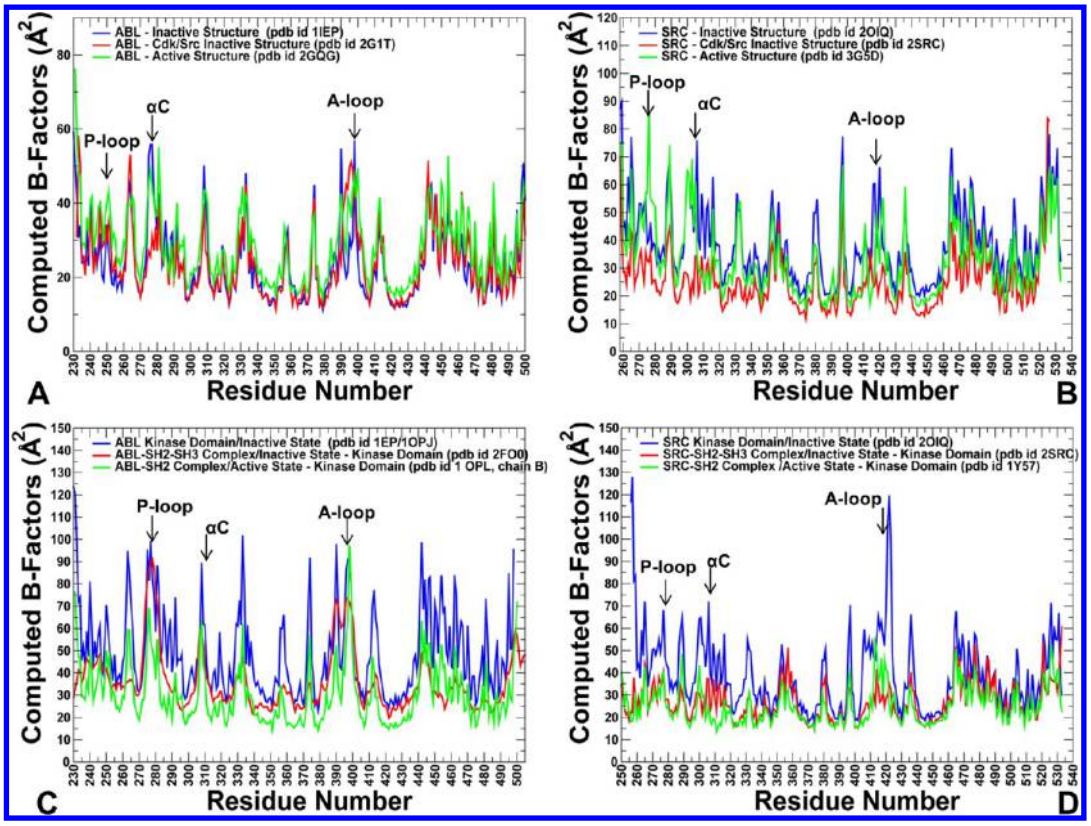

Figure 2. Conformational dynamics of the c-Abl and c-Src kinases. The computed B-factors obtained from MD simulations of the catalytic domains of c-Abl kinase (A) and c-Src kinase (B). The computed B-factors from MD simulations of the regulatory complexes are respectively shown for c-Abl (C) and c-Src (D). Equilibrium residue fluctuations of the catalytic domain are shown for the inactive structure (in blue), the Cdk/Src inactive structure (in red), and the active structure (in green). Equilibrium residue fluctuations of the inactive complex are in red and active complex in green. For comparison, the profile of the isolated catalytic core in the inactive state is shown in blue. Conformational mobility profiles of the P-loop, αC-helix, and A-loop are highlighted by arrows and annotated.

noncovalent edges (interactions). We found that the appropriate transition value for the cutoff I_{min} = 2.5%−3%. Hence, in the present study, any pair of residues are connected in the protein structure graph if I_{min} = 3.0%.

Global Network Parameters. A weighted network representation of the protein structure is adopted that includes noncovalent connectivity of side chains and residue cross-correlation fluctuation matrix.[83] In this model of a protein network, the weight w_{ij} of an edge between nodes i and j is determined by the dynamic information flow through that edge as measured by the correlation between respective residues. The weight w_{ij} is defined as $w_{ij} = -\log(|C_{ij}|)$ where C_{ij} is the element of the covariance matrix measuring the cross-correlation between fluctuations of residues is i and j obtained from MD simulations. The shortest paths between two residues are determined using the Floyd−Warshall algorithm[97] that compares all possible paths through the graph between each pair of residue nodes. Network calculations were performed using the python module NetworkX (http://networkx.github.io/). To select the shortest paths that consist of dynamically correlated intermediate residues, we considered the short paths that included sufficiently correlated (C_{ij} = 0.5−1.0) intermediate residues. Using the constructed protein structure networks, we computed the residue-based betweenness parameter. The betweenness of residue i is defined to be the sum of the fraction of shortest paths between all pairs of residues that pass through residue i:

$$C_b(n_i) = \sum_{j<k}^{N} \frac{g_{jk}(i)}{g_{jk}} \quad (3)$$

where g_{jk} denotes the number of shortest geodesics paths connecting j and k and $g_{jk}(i)$ is the number of shortest paths between residues j and k passing through the node n_i. Residues with high occurrence in the shortest paths connecting all residue pairs have a higher betweenness values. The normalized betweenness of residue i can be expressed as follows:

$$C_b(n_i) = \frac{1}{(N-1)(N-2)} \sum_{\substack{j<k \\ j\neq i\neq k}}^{N} \frac{g_{jk}(i)}{g_{jk}} \quad (4)$$

g_{jk} is the number of shortest paths between residues j and k; $g_{jk}(i)$ is the fraction of these shortest paths that pass through residue i.

RESULTS AND DISCUSSION

MD Simulations of c-Abl and c-Src Kinases: Dynamic Signatures of Functional States. Multiple crystal structures of the catalytic core and regulatory complexes were employed in MD simulations of c-Abl and c-Src kinases. The main goal of these simulations was to characterize conformational dynamics of the isolated catalytic domains and the effect of the SH3 and SH2 domains on dynamics of the catalytic core in the regulatory complexes. Using MD simulations we investigated how conformational dynamics of the c-Abl and c-Src catalytic

DOI: 10.1021/acs.jcim.5b00240
J. Chem. Inf. Model. 2015, 55, 1645−1662

domains and regulatory complexes can be related to differential sensitivity of these kinases to Imatinib binding. In this analysis, we tested a hypothesis that the conformational equilibrium of c-Abl for the isolated KD and the SH3-SH2-KD assembly may favor the specific inactive structure required for Imatinib binding. We show that a different thermodynamic balance of conformational states in c-Src kinase may be associated with more stringent energetic requirements for adopting the Imatinib-bound conformation. The following specific objectives were addressed in our simulations: (a) characterization of the intrinsic differences in conformational dynamics of the three major functional states in c-Abl and c-Src kinases; (b) determination of conserved signatures of the kinase dynamics in functional states and analysis of variations in structural stability of the critical "triad" (DFG motif, αC-helix, and A-loop); (c) analysis of dynamic coupling between structurally rigid and conformationally flexible regions that may be relevant for kinase regulation and activation.

The crystal structures of the catalytic core for c-Abl and c-Src kinases revealed three major functional states that were simulated in our study: the inactive conformation (DFG-out/αC-helix-in, A-loop closed),[38,39] the Cdk/Src-like inactive (DFG-in/αC-helix-out, A-loop closed),[40] and the active kinase form (DFG-in/αC-helix-in, A-loop open).[41] We found that the main regions of conformational flexibility in the c-Abl kinase domain included the αC-helix (residues 279−292) and the A-loop (residues 379−407) (Figure 2A). The glycine-rich P-loop (residues 248−255) displayed appreciable fluctuations only in the Cdk/Src inactive and active kinase conformations. We refer to residues according to the original numbering from the crystal structures (pdb id 1IEP and 2GQG).[38−41] Importantly, all functional kinase forms that were obtained from the crystal structures of the kinase complexes remained stable during MD simulations even in the absence of bound inhibitors. The inactive c-Abl conformation showed only small thermal variations in the key functional regions, owing to a stable kinked conformation of the P-loop and strong interactions formed between the P-loop and the A-loop (Figure 2A). In this inactive conformation, the A-loop tyrosine (Y393) is not phosphorylated and maintains a hydrogen bond with the catalytic aspartate D363. These interactions in the A-loop block the active site by mimicking the binding mode of substrates and may contribute to the stabilization of the inactive conformation. These observations are consistent with previous computational studies[51,52] confirming that the DFG-out inactive conformation in c-Abl can be structurally stable in the absence of bound Imatinib. At the same time, the Cdk/Src inactive conformation and active conformation were more flexible in the P-loop, the β4-β5 loop, the β3-αC loop, and A-loop. Despite structural similarity between the inactive structures of c-Abl and c-Src kinases, conformational dynamics of c-Src displayed a markedly different profile (Figure 2B). In this case, the Cdk/Src inactive structure emerged as the most stable kinase form, as evidenced from small fluctuations across the entire catalytic core, including the P-loop (residues 273−279), the αC-helix (residues 303−317), and A-loop (residues 403−425).

This residue annotation corresponds to the original residue numbering in the c-Src crystal structures (pdb id 2SRC, 2OIQ).[19,49] Of particular interest were the greater differences in thermal stability of c-Src states, suggesting a potentially higher energetic cost of conformational transitions from stable Cdk/Src form to the Imatinib-bound inactive state in c-Src.[51−54] To analyze functionally relevant motions in the c-Abl and c-Src structures we employed PCA of simulation trajectories.[94] Similarly to our previous studies,[93] we performed PCA of protein conformational dynamics based on the backbone heavy atoms (N, Cα, C$_\beta$, C, O) and the Cα atoms only that yielded very similar profiles. The three lowest eigenvectors captured ∼90% of the total variance in the collective motions derived from atomic fluctuations in each trajectory. In common to protein kinase domain folds, the first principal mode corresponded to the opening and closing movements of the N-terminal and C-terminal lobes, while in the second low frequency mode the kinase lobes produced a shear motion with a sliding movement along the interface between the N-terminal and C-terminal lobes.

Functional dynamics profiles in the essential space of the three lowest frequency modes were mapped onto c-Abl and c-Src structures and showed that structural rigidity of the catalytic core is coupled with conformational mobility and positional variability of the αC-helix and the P-loop (Figure S1, Supporting Information). The border between the rigid αC-β4 loop and a more flexible αC-helix defines a critical hinge site connecting regions of high and low structural stabilities in the catalytic domains of various kinases.[93] The intramolecular networks that form a regulatory spine (R-spine) and a catalytic spine (C-spine) networks connecting the N-lobe and the C-lobe are important for kinase regulation and activation.[6−11] Structural stability of the R-spine residues was shared across all c-Abl functional forms, even though the R-spine was partially disassembled in the inactive conformation. An important characteristic of c-Abl was a reduced mobility of the kinked P-loop in the DFG-out inactive conformation, whereas in a structurally similar c-Src structure this region was considerably more flexible.

The cross-correlation matrices of residue fluctuations along the low frequency modes displayed signs of long-range coupling between structurally stable kinked P-loop and the rest of the kinase core in the inactive c-Abl conformation (Figure S2, Supporting Information). On the other hand, a more flexible P-loop in the inactive form of c-Src may be only weakly coupled with the motions in other regions. A partially reduced mobility of the P-loop was also observed in the active c-Abl conformation (Figure 2A), while the P-loop remained to be highly mobile in the active c-Src form (Figure 2B). In general, the cross-correlation maps of residue fluctuations in the catalytic domain were indicative of more cooperative interaction networks in c-Abl conformations as compared to a rather loose pattern of correlated motions in c-Src kinase. These results indicated that subtle differences in the conformational dynamics of c-Abl and c-Src may be associated with different binding specificities of these kinases to Imatinib binding.

Conformational Dynamics of the Regulatory Complexes: Effect of SH3 and SH2 Domains on Structural Stability of the Catalytic Core. We also performed MD simulations of the c-Abl and c-Src regulatory complexes, particularly comparing equilibrium fluctuations of the catalytic core from simulations of the isolated KD and SH3-SH2-KD complexes. A central result of this analysis was the increased rigidity of the KD in the regulatory complexes as compared to simulations of the isolated KD (Figure 2C and D). We found that the SH3-SH2 interactions with the KD in the inactive kinase form could strengthen the autoinhibitory "lock" that effectively freezes the core domain in a conformation with low catalytic activity. Indeed, in the inactive c-Abl complex, the

DOI: 10.1021/acs.jcim.5b00240
J. Chem. Inf. Model. 2015, 55, 1645−1662

thermal fluctuations of the P-loop, A-loop, and αC-helix were especially small as conformational mobility of the KD appeared to be largely restricted (Figure 2C). A representative ensemble of conformational states for the dowregulated c-Abl complex (Figure 3A) could illustrate structural rigidity of the SH3 and

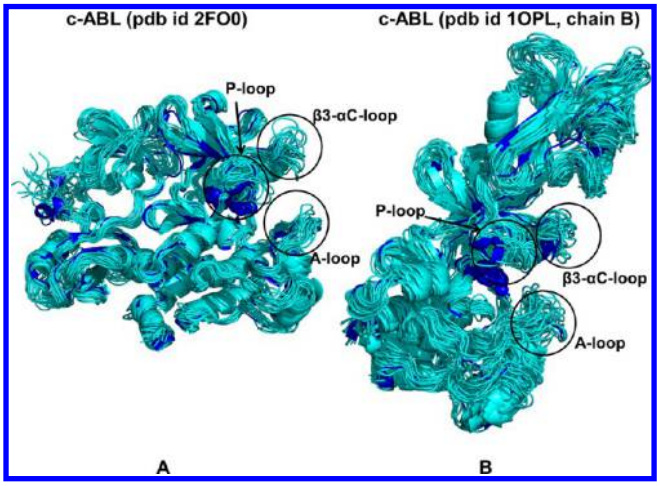

Figure 3. Conformational dynamics of the c-Abl complexes. An ensemble of 20 representative conformations extracted from equilibrium MD simulations of the autoinhibitory c-Abl complex (A) and active SH2-KD complex (B). Conformational fluctuations and positional variations of the SH3/SH2 domains as well as the P-loop, β3-αC loop, and the A-loop in the KD are highlighted.

SH2 domains as well as functional KD regions. Due to differences in the SH2 domain docking, the C-lobe of the c-Abl KD is rotated by approximately 20° relative to that in c-Src, resulting in a considerably tighter SH2-KD interface in c-Abl. This results in a more rigid inactive conformation of c-Abl KD in the autoinhibitory complex which may be more preferable by Imatinib as compared to c-Src conformation.

In a maximally activated "top-hat" conformation of the c-Abl core (Figure 3B), the regulatory complex undergoes a dramatic reshuffling, with the SH2 domain being completely reoriented and migrated to the top of the KD.[21,22] This rearrangement releases the autoinhibitory constraints by removing the SH2-SH3 lock and also allosterically enhances the kinase activity through SH2 binding with the N-terminal lobe of the catalytic core.[43,44] A similar domain rearrangement has been observed in regulatory complexes of Fes[24] and Btk kinases[98] in in which the SH2 domain acts as an allosteric modulator of the kinase activity. In simulations of the active complex, the SH2 domain binding considerably reduced conformational mobility of the N-lobe, including the P-loop (residues 266−275) and the αC-helix (residues 298−312). The release of the autoinhibitory constraints promoted some positional variations of the SH2 domain and facilitated concerted thermal fluctuations in the P-loop, β3-αC loop, and the A-loop (Figure 3B). In the active c-Abl complex, the P-loop moved away from the kinked orientation and assumed a more flattened position, thereby allowing the P-loop, β3-αC loop, and the αC-helix to move concertedly and form favorable interactions (Figure 3B). At the same time, the SH2 domain binding increased conformational mobility and accessibility of the A-loop (residues 396−420), likely due to cooperative influence of the P-loop and αC-helix. These observations are consistent with the recent biochemical studies,[44] according to which the SH2 domain can enhance accessibility of the A-loop to expose the Y412 residue for efficient phosphorylation and promote stabilization of the active structure. Hence, the SH2-KD interactions in the active c-Abl complex may reorganize the intrinsic dynamics of the catalytic domain and facilitate cooperative movements of the regulatory regions to promote stabilization of the catalytically competent state.

Noteworthy, the conformation and position of the SH3 domain in the active c-Abl complex was not determined in the crystal structure.[21] Moreover, the precise location of the SH3 domain could not be resolved even in a molecular envelope obtained by X-ray solution scattering,[22] although it was proposed that the SH3 domain may assume multiple conformations in solution by "sitting" on the top of the SH2 domain in a fully elongated structural arrangement of the core protein. As a result, computer simulations of the active c-Abl complex included the molecular assembly consisting only of the catalytic domain and the SH2 domain in the "top-hat" position with respect to KD. The role of the SH3 domain in the conformational dynamics and allosteric communications of the active c-Abl complex remain to be elusive and would require further structural characterization.

We similarly analyzed global motions in the c-Abl and c-Src regulatory complexes by computing conformational mobility profiles averaged over three lowest frequency modes. In the autoinhibitory complexes, the correlated domain movements were restricted in both c-Abl (Figure 4) and c-Src kinases (Figure 5). In a downregulated c-Abl form, the SH2 domain is more closely coupled with the C-lobe of the catalytic domain (Figure 4A). Conversely, in the inactive c-Src, the SH2 domain is more flexible and less restricted by its interactions with the C-lobe as the SH2-KD interface largely hinges on the engagement of the C-terminal tail pY527 residue with the SH2 domain (Figure 5A). In general, the SH3 and SH2 domains act concertedly in suppressing conformational mobility of the catalytic core in the inactive complexes by reducing collectivity of global movements. Hence, functional role of the SH2 and SH3 domains in constraining the downregulated kinase forms may be linked with the limited cooperative movements of the regulatory regions. In the crystal structure of the fully active complex,[21] the SH2 domain undergoes a significant reorientation by moving from the rigid autoinhibitory arrangement to a more dynamic top-hat arrangement. We found that the SH2 domain arrangement in the active c-Abl complex could induce significant correlations between the P-loop, the αC-helix, and the A-loop (Figure 4C,D). Collective displacements in these regions are directed toward stabilization of the active αC-helix position and improved coupling between the SH2 domain, the N-terminal KD lobe, and the open A-loop. A different structural arrangement of the active c-Src complex is associated with the SH3-KD positive coupling that can similarly facilitate collective motions of the P-loop, the αC-helix, and the A-loop toward the active positions (Figure 5C,D). We also noticed that the SH3-KD interactions may induce cross-correlations and long-range coupling between the SH3 domain and the N-terminal lobe residues beyond the immediate interface.

Network Analysis of c-Abl and c-Src Kinase Domains: Inferring Binding Preferences from Residue Centrality. Analysis of MD trajectories and equilibrium fluctuations could provide only an initial and mostly qualitative outlook of relative stability of different functional states in c-Abl and c-Src kinases. We combined the results of MD simulations with the structure-based network analysis to determine evolution of the residue interaction networks in different conformational forms of c-Abl

DOI: 10.1021/acs.jcim.5b00240
J. Chem. Inf. Model. 2015, 55, 1645−1662

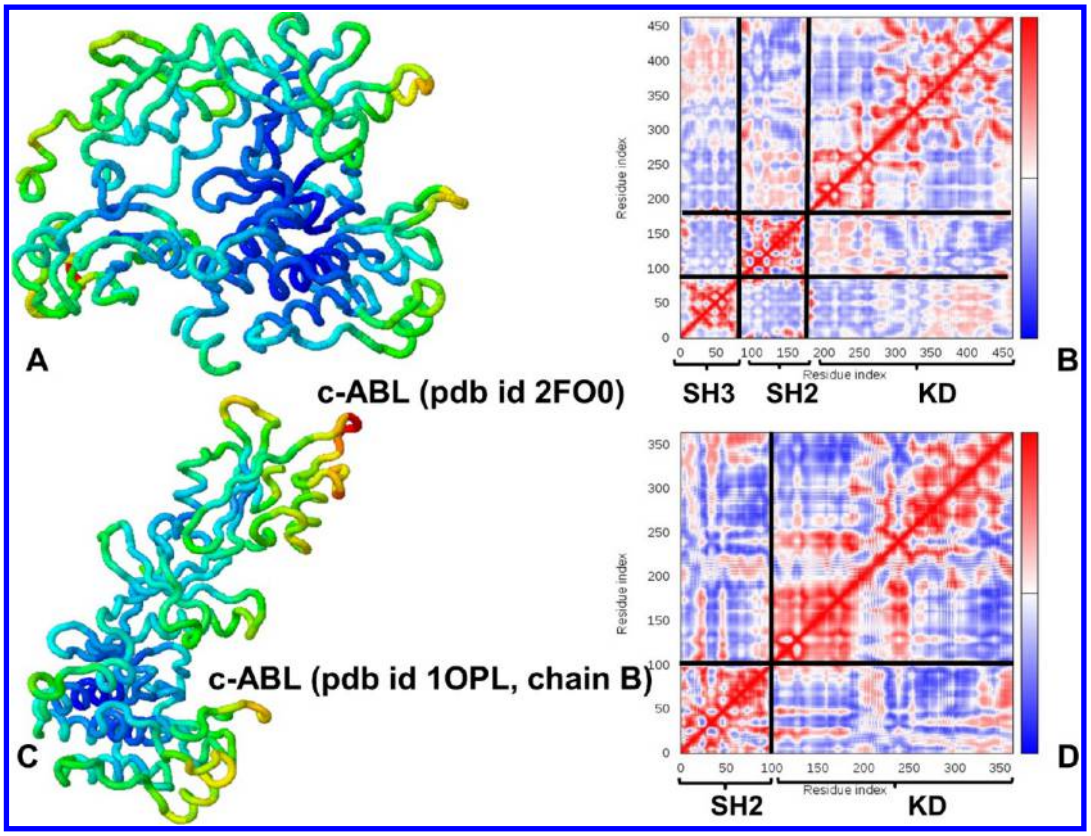

Figure 4. Analysis of correlated motions in the c-Abl complexes. Conformational dynamics profiles of the c-Abl complexes (A,C) and cross-correlation matrices of residue fluctuations along the low frequency modes (B,D). Conformational dynamics profiles were computed by averaging protein motions in the space of three lowest frequency modes. The color gradient from blue to red indicates the decreasing structural rigidity of the protein residues. PCA computations are based on the Cα atoms. The axes denote Cα atoms of the protein residues in sequential order. Cross-correlations of residue-based fluctuations vary between +1 (fully correlated motion; fluctuation vectors in the same direction, colored in red) and −1 (fully anticorrelated motions; fluctuation vectors in the same direction, colored in blue). The residue ranges corresponding to the SH3, SH2, and KD are highlighted.

and c-Src kinases. Protein structure networks were constructed by incorporating the topology-based residue connectivity in combination with the contact maps of residues cross-correlations obtained from MD simulations.[83] This approach is conceptually similar to an integrated approach[85,99] that combined solution NMR and chemical shift titrations data with the mutual information and community network analysis to determine ensembles of allosteric communication pathways. We use similar principles to construct ensemble-based residue interaction networks as we integrated cross-correlations of residue motions a guiding indicator of allosteric communications in conformational ensembles. Noteworthy, there are some technical distinctions between these approaches as the earlier study[85] considered only heavy atoms to build protein network connectivity, with the edge lengths being weighted by the mutual information correlation of each pair of residues. In our investigation, a more detailed side-chain model of noncovalent residue connectivity is employed and the edges are weighted according to the cross-correlations between residue fluctuations during unbiased all-atom simulations. Common to methods, a global network parameter, residue betweenness, was used to characterize the topology and dynamics of the residue interaction networks in functional kinase states. The betweenness of a node is defined as the number of shortest paths that pass through that node in the network, representing a global centrality measure of the node contribution to the network. Throughout the text, we interchangeably use terms "residue centrality" and "residue betweenness".

According to our primary conjecture, structural stability of conformational kinase states may be determined by the organization of the residue interaction networks and distribution of highly connected residues in the regulatory regions. We proposed that functional significance of kinase residues in regulation may be linked with their network signatures and specific structural role as global mediating sites of allosteric interactions. To test this hypothesis, we first computed MD-averaged residue betweenness profiles for different conformational states of the c-Abl and c-Src catalytic domains. A central result of this analysis is that residues that are indispensable for Abl kinase regulation and catalysis corresponded to the high centrality nodes and can be clearly distinguished by their specific network signatures. In c-Abl kinase, the residue betweenness in the Imatinib-bound inactive structure was on average higher than in the Cdk/Src inactive conformation and the active kinase form (Figure 6A), likely reflecting the greater structural stability of this functional form. These findings are in line with the recent evidence that the isolated Abl KD thermodynamically favors a "closed" DFG-out conformation.[44] A markedly high betweenness was observed for the following binding site residues in the Imatinib-bound conformation: P-loop residues (L248 and Y253), a catalytic pair (K271, E286), αC-β4-loop/αC-helix residues (M290, I293), the gate-keeper residue T315, D363 (HRD catalytic motif), and Y393

DOI: 10.1021/acs.jcim.5b00240
J. Chem. Inf. Model. 2015, 55, 1645−1662

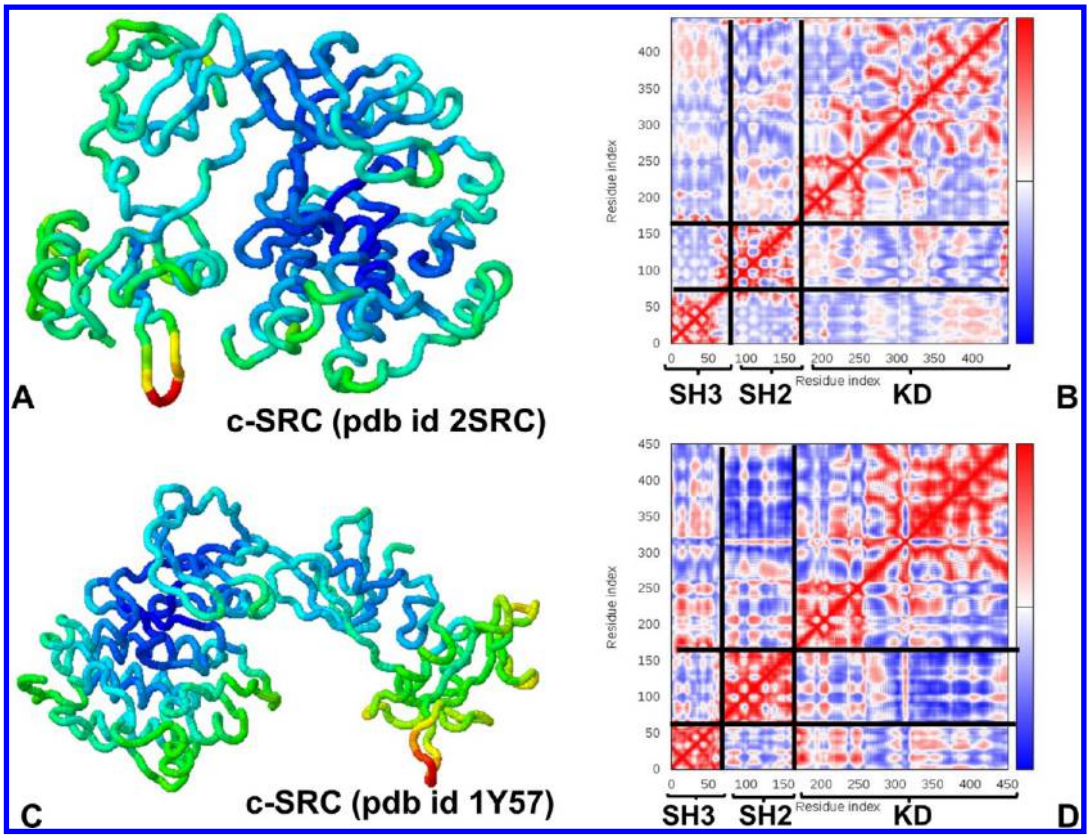

Figure 5. Analysis of correlated motions in the c-Src complexes. Conformational dynamics profiles of the c-Src complexes (A,C) and cross-correlation matrices of residue fluctuations along the low frequency modes (B,D). Conformational dynamics profiles were computed by averaging protein motions in the space of three lowest frequency modes. The color gradient from blue to red indicates the decreasing structural rigidity of the protein residues. PCA computations are based on the Cα atoms. Cross-correlations of residue-based fluctuations vary between +1 (fully correlated motion; fluctuation vectors in the same direction, colored in red) and −1 (fully anticorrelated motions; fluctuation vectors in the same direction, colored in blue). The residue ranges corresponding to the SH3, SH2, and KD are highlighted.

(phosphorylation site in the A-loop) (Figure 6B). From structural perspective, this may reflect the integrating role of Y253, D363, and Y393 residues in stabilizing allosteric interaction networks between the kinked P-loop, catalytic core, and unpohosphorylated A-loop of c-Abl.

Intriguingly, these findings indicated that structural stability of the inactive c-Abl conformation may be dependent on the precise structural positions and allosteric coupling between high centrality residues Y253, D363, and Y393. The strategic position of Y393 and its integrating central role is consistent with the high sensitivity of Imatinib binding to the specific DFG-out conformation and an obligatory unphosphorylated status of Y393 in this structure. Indeed, phosphorylation of Y393 is known to stabilize the active c-Abl conformation, thus blocking the Imatinib entrance to the catalytic region and severely compromising its inhibitory function.[33,42] Hence, the unique networking characteristics of these residues may be relevant in relating the high sensitivity of Imatinib to the kinked P-loop conformation and an obligatory unphosphorylated form of the A-loop in c-Abl.

A different balance between conformational states was seen in c-Src kinase, where the centrality profiles revealed the higher residue connectivity in the Cdk/Src conformation (Figure 7A). The high centrality residues included the V313, M314 (αC-helix), L317, L322, V323 (αC-β4-loop), and L407, L410, E412 (A-loop) (Figure 7B). A tight local module of structurally rigid residues in the αC-β4-loop/αC-helix region (V313, M314, L322, V323) is connected with the A-loop local cluster (L407, L410, Y426, F424) leading to stabilization of the αC-helix-out conformation in the Cdk/Src-like inactive kinase form. Despite structural similarities between the Imatinib-bound states, the betweenness of the P-loop residues, particularly F278 (Y253 in c-Abl), was reduced due to the increased mobility and decoupling of the P-loop motions from the rest of the catalytic core. Hence, relatively small differences in the residue interaction networks of c-Abl and c-Src may affect global coordinating role of functional residues.

We specifically highlighted differences in the centrality profiles of the binding site residues across functional states of c-Abl and c-Src kinases (Figure 8). In c-Abl kinase, betweenness values (Figure 8A) of the Imatinib-interacting residues were greater in the inactive conformation than in the Cdk/Src state, especially for Y253, T315 residues as well as the HRD and DFG motifs. In other words, the Imatinib-interacting residues in the inactive c-Abl structure may be preorganized for Imatinib binding. In this context, Imatinib may choose the inactive c-Abl state using conformational selection mechanism to preferentially bind with the highly connected and stable binding site residues.[100] Conformational selection of the inactive Abl state may be then accompanied by the inhibitor-induced stabilization of this functional form via an induced fit. In this scenario, the steric barrier for the movement away from the Imatinib-bound inactive state can be increased that would effectively lock the kinase in a specific conformation. Hence, Imatinib selectivity may result from ligand-induced network stabilization of the inactive c-Abl structure—a mechanism which combines an

DOI: 10.1021/acs.jcim.5b00240
J. Chem. Inf. Model. 2015, 55, 1645−1662

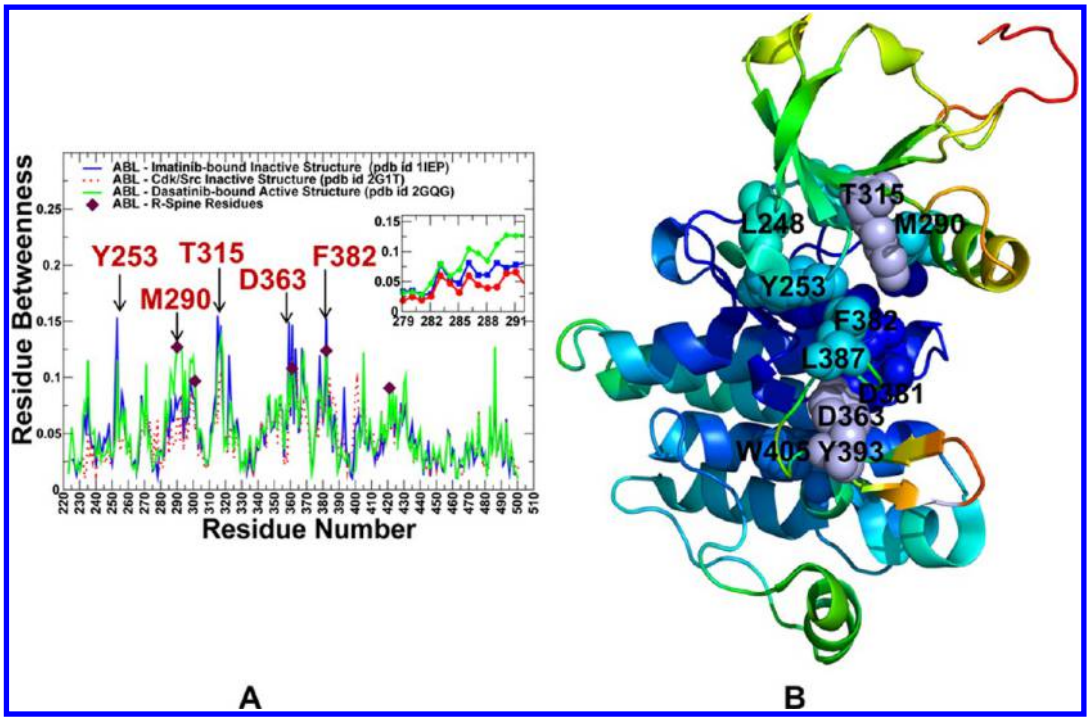

Figure 6. Residue-based centrality analysis of c-Abl KD conformations. (A) Residue-based betweenness profiles of c-Abl structures are shown for the Imatinib-bound inactive conformation (in blue), Cdk/Src inactive conformations (in red), and the active structure (in green). A close-up view of the αC-helix profiles (residues 279−292 according to the residue numbering in the crystal structures 1IEP/2GQG is provided as an inset. The R-spine residues (L301 from the β4-strand, M290 from the αC-helix, F382 of the DFG motif, H361 of the HRD motif, and D421 of the αF-helix) are shown by filled maroon-colored diamond symbols. (B) Structural mapping of the high centrality residues onto the inactive c-Abl conformation (pdb id 1IEP). The annotated c-Abl residues included L248 in β1/P-loop, Y253 in the P-loop, catalytic pair K271/E286, M290, I293 (αC-helix), gate-keeper T315, D381 (HRD), F382 (DFG), L387 (A-loop), Y393 (A-loop), W405 (substrate binding region 405-WTAPE-409).

induced fit and conformational selection models. At the same time, the network signatures of the binding site residues in c-Src kinase were considerably different. The centrality of the binding site residues in the Cdk/Src inactive conformation was noticeably higher than in the Imatinib-bound inactive (Figure 8C) and the active states (Figure 8D). According to our model, the greater structural stability of the Cdk/Src inactive form may impose stricter energetic requirements for adopting the Imatinib-bound conformation in c-Src kinase and contribute to the weak Imatinib binding with c-Src kinase. These results provide a network-based framework in explaining mechanisms of differential kinase sensitivity to Imatinib, supporting conclusions reached in recent computational[54−56] and experimental investigations.[57]

Network Organization of the Regulatory Complexes: Spatially Separated High Centrality Residues Mediate Stabilization of the Catalytic Core. Through characterization of the network organization in functional kinase assemblies, we investigated allosteric mechanisms by which the SH3 and SH2 domains may exercise their regulatory control over the catalytic domain and kinase activity. To evaluate the effect of the SH3 and SH2 domains, we first compared the residue-based centrality profiles of the catalytic domains obtained from simulations of the isolated KD forms and SH3-SH2-KD complexes. We found that the network centrality of KD residues generally increased in the autoinhibitory complexes relative to the corresponding values in the isolated KD (Figure 9A and C). The average residue centrality in the catalytic domain increased even more drastically in the active complexes (Figure 9B and D), suggesting that the SH3-SH2-KD interactions play key role in coordinating conformational equilibrium and kinase activation. The observed network changes were especially pronounced in the c-Abl downregulated complex, reflecting a tight SH2-KD interface and the increased structural stability of the inactive KD conformation (Figure 9A). In particular, we detected a sharp increase in centrality of the HRD and DFG-out motifs, including H380 (380-HRD-382) and F401 (400-DFG-402). Note that this annotation of the c-Abl KD residues corresponds to their numbering in the SH3-SH2-KD c-Abl complex (pdb id 2FO0). As a result, the SH3-SH2 interactions may rigidify the inactive DFG-out conformation that is required for productive Imatinib binding. Similarly, the autoinhibitory interactions in the downregulated c-Src complex resulted in the increased centrality of the KD residues in the Cdk/Src inactive conformation (Figure 9C). These results supported the notion that the intrinsic predisposition for specific and different inactive KD conformations in c-Abl and c-Src complexes may contribute to the preferential Imatinib inhibition of c-Abl.[101]

Of special interest was the dramatically increased residue centrality in the active c-Abl complex (Figure 9B). In particular, the SH2 residues I164, R185, T231, and Y234 corresponded to the distribution peaks, suggesting that these residues could mediate long-range allosteric signaling in the active complex. Remarkably, these high centrality sites are critical for stabilization of the active structure and regulation of kinase activity. In fact, targeting of the SH2-kinase interface by a single I164E mutation appeared to cause a dramatic reduction in transformation and loss of leukemogenesis due to disruption of the SH2-kinase.[43] Moreover, autophosphorylation of Y412 of the A-loop, which is a signature of the activated state, could be strongly decreased in the I164E mutant and is completely

DOI: 10.1021/acs.jcim.5b00240
J. Chem. Inf. Model. 2015, 55, 1645−1662

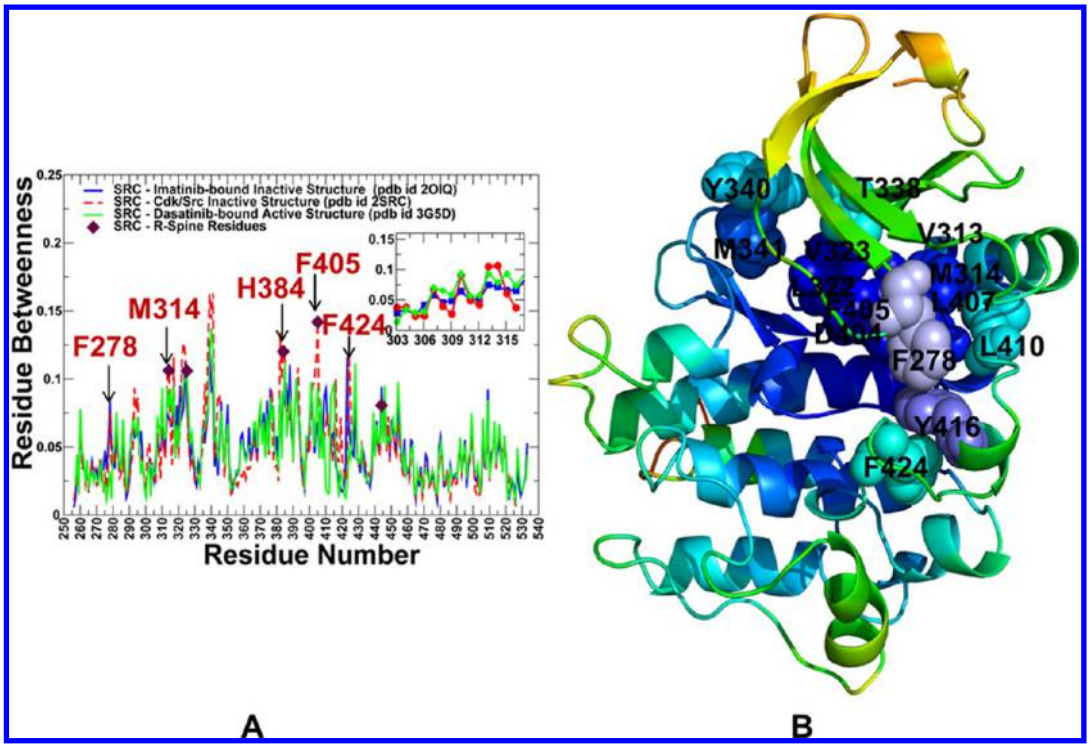

Figure 7. Residue-based centrality analysis of c-Src KD conformations. (A) Residue-based betweenness profiles of the c-Src structures are shown for the Imatinib-bound inactive form (in blue) and Cdk/Src inactive conformation (in red) and the active structure (in green). A close-up view of the αC-helix profiles (residues 303−317 according to the residue numbering in the crystal structures 2OIQ/3G5D is provided as an inset. The R-spine residues (M314, L325, H384, F405, and D444) are shown by filled maroon-colored diamond symbols. (B) Structural mapping of the high centrality residues onto the Cdk/Src inactive conformation (pdb id 2SRC). The annotated c-Src residues and respective functional regions included F278 (P-loop), binding site hinge residues (gate-keeper T338, Y340, M341), V313, M314 (αC-helix), L322, V323 (αC-β4-loop), D404, F405 (DFG motif), L407, L410, Y416, F424 (A-loop).

abolished with the introduction of additional S162 K mutation at the SH2-KD interface.[43,44] The importance of the SH2 residues T231 and Y234 as global mediating sites in the active complex was also evident in functional studies.[48]

Importantly, we found that the SH2-KD interactions in the active c-Abl complex may have a significant long-range effect on structural stability of the KD residues that extends beyond the immediate SH2-KD interface. A strong allosteric effect on the catalytic core was manifested in the increased connectivity of the N-lobe residues, including the P-loop (residues 266−275) and the αC-helix (residues 298−312). Additionally, the SH2-KD interactions increased stability of the interfacial residues, including the N-lobe residues (K290, T291, and L292). We also noticed that high centrality of key functional residues from the catalytic domain was preserved in the regulatory complex, including T334 (gate-keeper), H380 (HRD), D400, and F401 (DFG). A partial redistribution of the mediating KD residues may be dictated by functional requirements to reduce distortions in the N-terminal lobe and stabilize active positions of the P-loop and αC-helix. These allosteric changes may be necessary for efficient phosphorylation of Y412 and stabilization of the catalytically competent state.

Functional Significance of High Centrality Residues in the Regulatory Complexes: The Network Signatures of Phosphorylation Sites. According to the main premise of this work, the network topology and distributions of high centrality residues in the regulatory complexes may reflect the underlying mechanism of allosteric signaling, describe the molecular details of kinase regulation and specify the coordinating role of functional residues. By analyzing residue interaction networks in the SH3-SH2-KD complexes, we identified high centrality sites where mutations and/or structural perturbations may affect regulatory interactions and potentially induce large conformational rearrangements. The central result of this analysis is that high centrality residues corresponding to the distribution peaks can unambiguously pinpoint essentially all functional sites that are known to be important in regulation of kinase activity.[22,23] Most notably, the majority of high centrality residues in the SH3 and SH2 domains corresponded to the tyrosine residues whose mutations and phosphorylation status are known to regulate c-Abl activity. Indeed, the high centrality peaks included c-Abl residues from the SH3 domain (Y89, Y134, S94, W118), the SH2 domain (E157, Y158), SH2-kinase linker (K241, P242, Y245, P249), and KD residues (H314, T334, H380, R386, F401) (Figure 10 A). In network terms, it implies that phosphorylation of these highly connected tyrosine sites could simultaneously disrupt multiple autoinhibitory contacts and thus compromise stability of the downregulated complex. Our results are consistent with a range of mutagenesis studies that established functional role of these residues for kinase regulation. In particular, it was demonstrated that the SH2 domain mutations E157A and Y158D[13] and W118A mutation in the SH3 domain as well as the linker double PP mutation P242E/P249E[32,33] can upregulate Abl activity.

Network analysis of c-Src complexes identified a set of conserved, high centrality residues that may be involved in mediating interaction networks in different structural contexts of the inactive and active complexes (Figure 11). In the autoinhibitory complex, the high centrality sites included the

DOI: 10.1021/acs.jcim.5b00240
J. Chem. Inf. Model. 2015, 55, 1645−1662

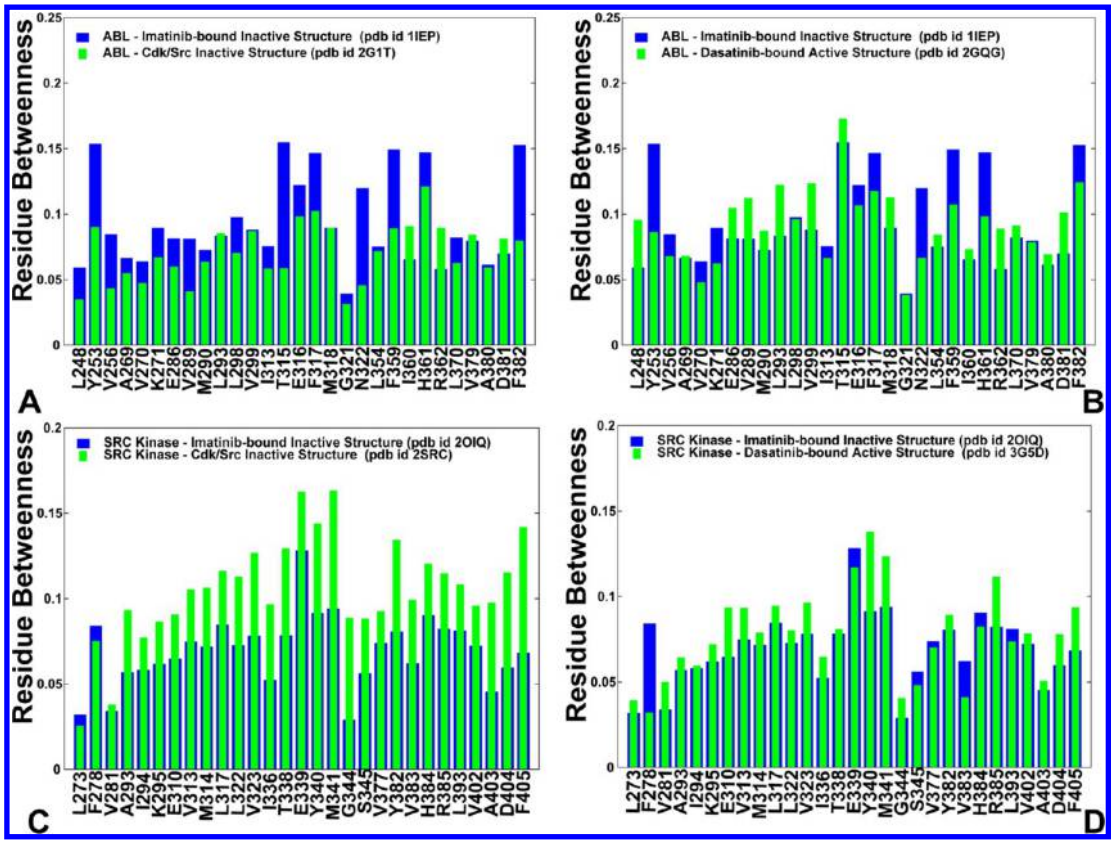

Figure 8. Comparative analysis of the betweenness profiles for the inhibitor interacting residues. The differences in the betweenness profiles of the inhibitor-interacting residues across functional states of c-Abl and c-Src kinases are shown in colored bars. A comparison of the betweenness profiles for the Imatinib-interacting residues is shown for the inactive and Cdk/Src inactive c-Abl conformations (A) and for the inactive and active c-Abl conformations (B). A similar comparison is presented for c-Src conformational states (C,D). Note that the binding site residues in the inactive c-Abl structure have a high level of betweenness in the absence of Imatinib. The betweenness of the binding site residues in c-Src kinase showed that these residues are more stable in the Cdk/Src inactive conformation.

SH3 residues (Y92, W118, Y136), the SH2 residues (R175, R155, E157, R160), and the SH2 linker residues (T252, L255, W260) as well as the R-spine residues in the KD (M314, L325, H384, F405). Functional significance of these high centrality residues in c-Src was validated in various biochemical experiments. In particular, mutations in the interface between the αC-helix and the A-loop such as M314A, L410A, and E412A may result in deregulated kinase as it would disrupt a specific autoinhibitory arrangement in c-Src kinase.[102] The W260A mutation of the mediating linker residue W260 destabilizes the intramolecular interactions that maintain the inactive conformation.[103] The L255 residue is another critical component of the intramolecular inhibition mechanism of Src family kinases[104] as mutations in of this hydrophobic residue can completely deregulate Src activity. Strikingly, these two hydrophobic residues in the SH2 linker emerged as strong centrality peaks in both inactive and active complexes, pointing to their global mediating role in allosteric interaction networks. As a result, their mutations may perturb global communication between the SH2 domain, the N-terminal lobe and the αC-helix in the catalytic domain. This network-based interpretation may rationalize why even minor mutations in these positions may render significant changes in kinase activity. Our results could also clarify the originally proposed mechanism, according to which the length and bulkiness of L255 residue may be precisely tailored for the efficient signal transmission from the SH2 and SH3 domains to functional regions in the catalytic core, particularly to modulate conformational movements of the αC-helix.[104]

The network analysis of c-Src conformations was particularly interesting in light of structural and mutational analysis showing the increase in the Imatinib affinity to c-Src upon L407G mutation (~8 fold) and L407G/W260A (~15 fold).[49] These mutations were specifically designed to destabilize the inactive Cdk/Src conformation of c-Src and showed a detectable improvement in the Imatinib binding affinity. According to our data, mutations of these high centrality residues may destabilize the interaction networks in the autoinhibited c-Src conformation leading to redistribution of conformational states and potentially tipping the dynamic equilibrium toward the Imatinib-bound, inactive conformation.

A natural question is whether network centrality is a unique signature of regulatory sites in the kinase complexes. We also evaluated several other residue-based structural parameters, such as local residue flexibility, residue-based relative solvent accessibility (RSA),[95] and residue depth.[96] The residue betweenness was fairly well correlated with local conformational fluctuations (Figure S3, Supporting Information). Hence, highly connected central residues in regulatory complexes are mostly rigid and may experience small concerted fluctuations with the rest of the protein. Despite a strong correlation pattern, structural rigidity may not necessarily imply high centrality as residues with low B-factors may display medium and high betweenness values. The RSA and betweenness

DOI: 10.1021/acs.jcim.5b00240
J. Chem. Inf. Model. 2015, 55, 1645−1662

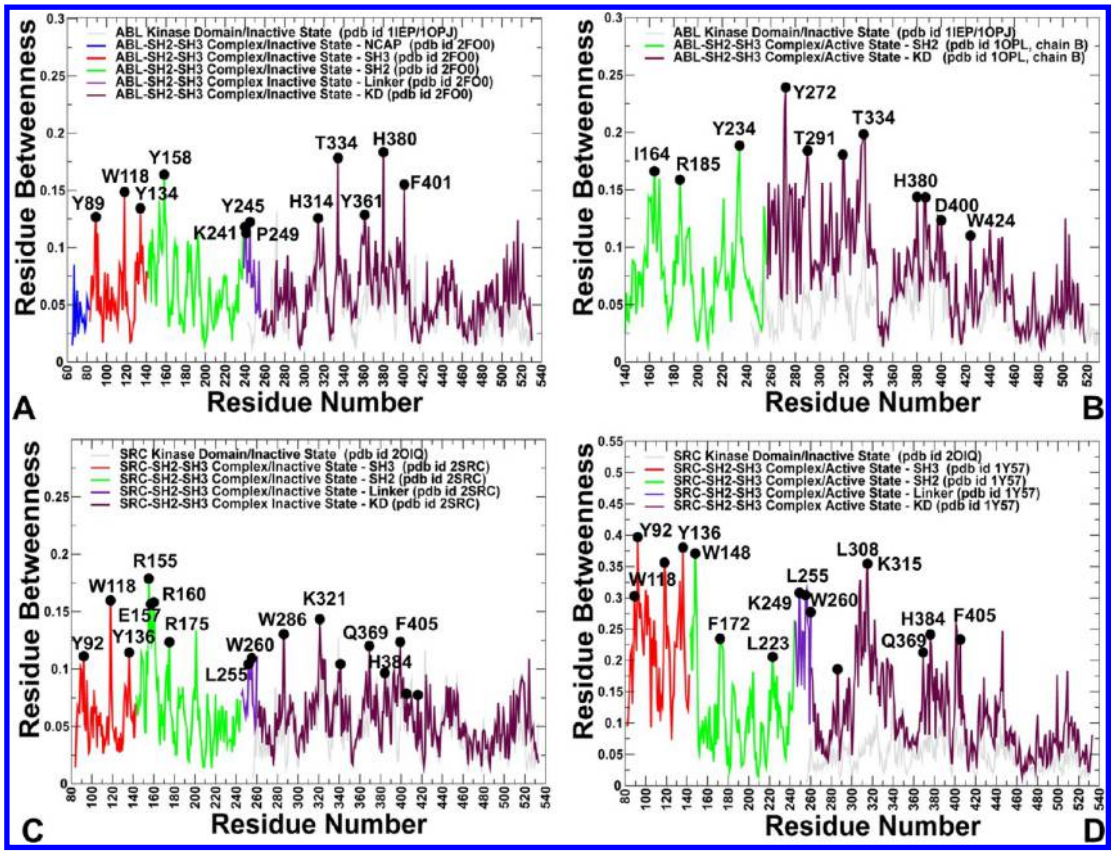

Figure 9. Residue-based centrality analysis of c-Abl and c-Src regulatory complexes. The residue betweenness profiles are shown for the autoinhibitory c-Abl complex (A), active c-Abl complex (B), inactive c-Src complex (C), and active c-Src complex (D). The centrality values of different domains are respectively shown for SH3 (in red), SH2 (in green), SH2 linker (magenta), and KD (maroon). For reference and comparison, the residue centrality profile of the isolated KD structures is also shown (in gray). The betweenness values are obtained by averaging network computations over the MD trajectories of the kinase complexes. The high centrality residues are annotated and shown by filled maroon circles.

parameters were generally correlated, showing that highly connected and stable residues would likely to reside in a locally buried structural environment and "poor" centrality was mostly associated with solvent-exposed (high RSA values) residues (Figure S4, Supporting Information). By mapping functionally important for regulation residues in c-Abl and c-Src complexes onto the respective RSA profiles (Figure S5, Supporting Information), we observed that these sites have generally low RSA values and could be largely shielded from solvent. However, the bulk of protein residues in regulatory complexes have similar or lower RSA values. Although residue depth of functional residues is above the average value, this metric may also be insufficiently robust to differentiate global mediating sites from surrounding residues (Figure S6, Supporting Information).

This analysis highlighted an important fact that global measures of residue contributions to the interaction networks may provide a simple and robust indicator of functional significance for kinase regulatory mechanisms. Combining local measures of residue flexibility and solvent accessibility with global centrality parameters may describe complementary features and potentially yield a more accurate and detailed characterization of structural stability at the residue and protein levels.

High Centrality Sites Are Linked in Communication Pathways: A Mechanism to Balance Efficiency and Robustness of the Interaction Network. To understand mechanistic basis for signal transmission in the regulatory kinase assemblies, we also modeled allosteric communication pathways by utilizing the computed ensembles of short paths between any pair of residues in different functional forms. Using this approach, we tested a conjecture that highly connected and structurally stable residues can be linked to each other to form a "chain" of functional sites involved in a rapid and robust propagation of allosteric effects. Specifically, we analyzed how allosteric signals may be transmitted from the interdomain interfaces to the phosphorylation site Y412 in the A-loop of c-Abl kinase. In the downregulated c-Abl complex, communication routes connecting phosphorylation sites in the SH3 and SH2 domains with KD often pass through Y245 in the SH2-linker and then connect to H314 and I312 (αC-β4 loop/αC-helix; Figure 10A). Optimal pathways would then proceed to the R-spine M309 (αC-helix) and via D400 and F401 (DFG motif) reach out to the H380, R381 (HRD), and finally to Y412. In the active c-Abl complex, an efficient and robust communication pathway can directly connect high centrality residues I164 (SH2 domain) with T291 and K290 (N-lobe of KD) and, then, via a catalytic pair K290-E405 proceeding to F401 (DFG), H380, and R381 (HRD) finally reaching out to Y412 (Figure 10B). Another efficient pathway may direct signaling from F401 to R386 and 424-WTAPE-428 motif that anchors the substrate binding P + 1 loop to the αF-helix, providing a plausible route for signal communication to allosteric binding site (Figure 10B). As a result, the DFG motif may serve as a main "dispatcher" in the catalytic domain

DOI: 10.1021/acs.jcim.5b00240
J. Chem. Inf. Model. 2015, 55, 1645−1662

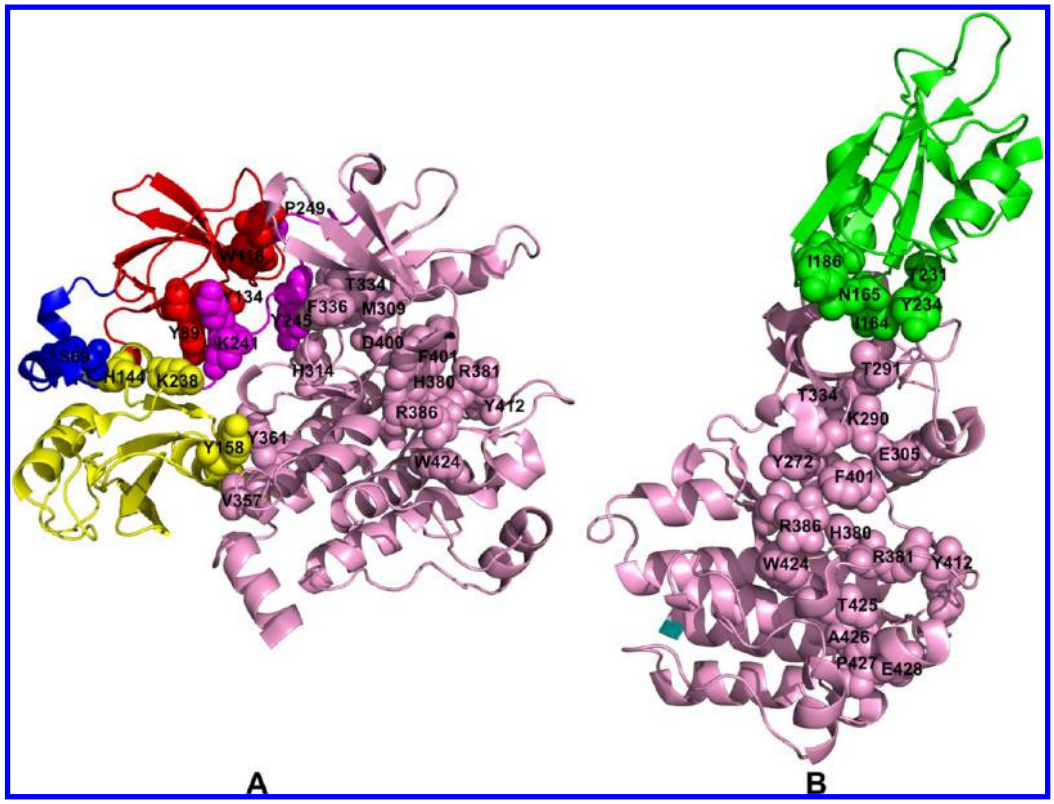

Figure 10. High centrality sites and conformational allosteric pathways of the c-Abl complexes. The high centrality residues in the downregulated c-Abl (A) and active c-Abl complexes (B) are mapped onto the respective crystal structures (pdb id 2FO0 and 1OPL, chain B). An optimal allosteric pathway between the SH2 linker (Y245) and phosphorylation site Y412 in the inactive complex involves the following residues: Y245, H314, I312, M309, T334, D400, F401, H380, R381, and Y412 (A). In the active complex, a communication route between the SH2-KD interface I164 and Y412 proceeds via I164, T291, K290, E405, F401, H380, R381, Y412. The allosteric pathways are based on the constructed protein structure networks and are determined as the shortest paths between two given residues. The residues are shown in colored spheres according to their domain identity consistent with annotation in Figure 1: SH3 (red), SH2 (green), SH2 linker (magenta), and KD (pink).

that directs communication signals from the SH3 and SH2 domains to different functional regions.

A central observation emerged from this analysis is that highly connected residues would more likely to link with other highly connected residues, thus forming rapid and resilient communication paths. The preferred communication between hubs with similar connectivity level is often referred in the network science as the "rich-club" phenomenon.[105] Hence, high centrality residues may link to each other and exhibit so-called assortativity, i.e. the propensity for preferential attachment with nodes of similar centrality.[106] According to this mechanism, high centrality residues involved in transmission of allosteric signals may be supported by neighboring nodes that provide functional redundancy and sufficient robustness to failures caused by random or targeted mutations.

Two Conserved Linker Residues Mediate Allosteric Communications in c-Src Complexes. Modeling of allosteric pathways connecting the SH3 and SH2 domains with the catalytic core showed that high centrality residues can be linked to each other forming efficient communication routes, in which two residue in the SH2 linker (L255 and W260) may serve as "central dispatchers" that control signaling. The SH3 domain tyrosine residues Y92 and Y136 form an interaction cluster with T252 of the linker, while W118 (SH3 domain) makes multiple contacts with L255 and W260 (linker) (Figure 11A). Direct interactions formed by the SH3 domain (W118) with the linker are communicated via L255 and W260 to the N-terminal lobe of the catalytic domain. Optimal pathways connect W260 residue with the R-spine residues in the αC-helix residues (M314, L325) and short helix in the A-loop (L407) reaching out to F405 (DFG), H384, R385 (HRD), and Y416 (Figure 10A). Hence, efficient and short communication routes between the SH2 linker and phosphorylation site in the A-loop prefer to navigate through a network of conserved and structurally rigid residues that contribute to stabilization of the inactive αC-out conformation that blocks the formation of the catalytic salt bridge required for activation. Despite structurally different arrangement of the active complexes we observed a similarly strong allosteric effect of the SH2 and SH3 domains on the catalytic core in the active c-Src complex. The connectivity and structural stability of the N-lobe residues significantly increased, with changes being especially pronounced for the αC-helix (residues 303−327). The key residues in the catalytic core (384-HRD-386 and 404-DFG-406) retained their strategic role in the active complex and attained higher betweenness values. Among high centrality sites in the active complex are also linker residues L255 and W260 that could mediate stable interaction networks and communication paths in the inactive and active complexes. Most of the interdomain "traffic" in communication pathways is dispatched through L255 that directly interfaces with L308 (αC-helix) and then via catalytic E310 residue connects with the KD residues F405, H384, and R385 reaching to the phosphorylation site Y416 (Figure 10B). Another communication hub is W260 residue that interfaces with K315 and then connects with the R-spine M314 to follow the same short path (E310, F405, H384,

DOI: 10.1021/acs.jcim.5b00240
J. Chem. Inf. Model. 2015, 55, 1645−1662

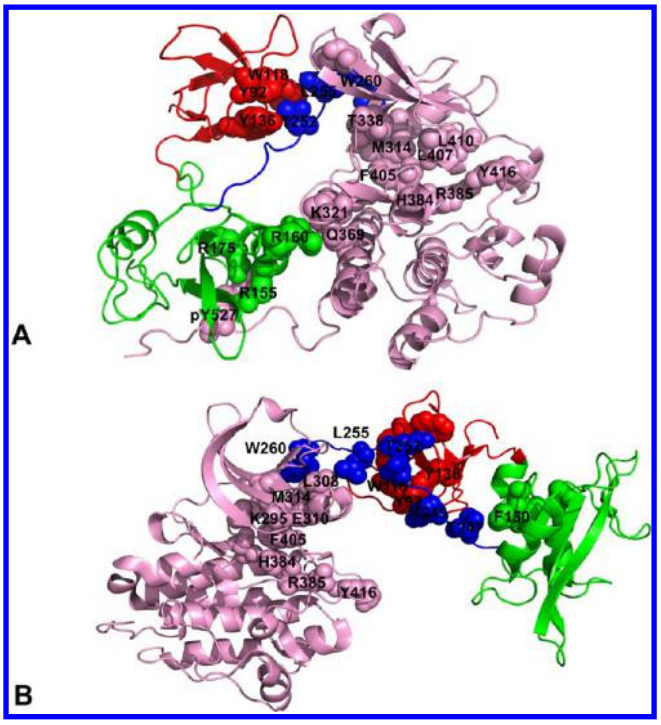

Figure 11. High centrality sites and conformational allosteric pathways of the c-Src complexes. The high centrality residues in the downregulated c-Src (A) and active c-Src complexes (B) are mapped onto the respective crystal structures (pdb id 2SRC and 1Y57). In the inactive complex, the optimal pathway connecting the SH3 domain with the phosphorylation site in the A-loop (Y416) includes Y92, Y92, W118, Y136, L255, W260, W286, M314, L325, F405, H384, R385, and Y416. In the active complex, the optimal pathways consist of W260, L255, L308, E310, F405, H384, R385, and Y416. The residues are shown in colored spheres according to their domain identity consistent with annotation in Figure 1: SH3 (red), SH2 (green), SH2 linker (magenta), and KD (pink).

R385) reaching to the final destination Y416 residue in the A-loop. Our results may therefore provide an insight into the experimentally known regulatory role of L255 and W260 residues.[103,104] These conserved residues in the SH2 linker mediate the allosteric effect of the SH3 and SH2 domains on the catalytic core of c-Src. In summary, we found that the network of high centrality residues may act as a direct path for transmitting signals between allosterically coupled regions.

CONCLUSIONS

We have presented a comprehensive platform of network-based approaches that were integrated with biophysical simulations and computational modeling to gain insight into organizing principles of the residue interaction networks that underlie mechanisms of kinase activity and specificity. We focused on the network-based modeling of differential sensitivity and binding specificity in c-Abl and c-Src kinases to drug binding. Our results have shown that Imatinib binding preferences toward the c-Abl kinase may result from subtle thermodynamic balance of conformational states and ligand-induced network stabilization of the inactive c-Abl structure—a mechanism which combines an induced fit and conformational selection models. A classic paraphrase of famous Tolstoy's quote in relationship to a protein kinase universe[2] stated that "All active kinases are alike but an inactive kinase is inactive after its own fashion." While the active conformations of protein kinases indeed closely resemble one another, it appeared that specific inactive structures of c-Abl and c-Src kinases may be also very similar, and their markedly different response to Imatinib may be associated with the unique networking signatures. This study has revealed that network centrality can unambiguously distinguish functional sites responsible for regulatory interactions in the autoinhibitory and active complexes. Structure-based network analysis has also recapitulated a broad range of mutagenesis data by linking residue centrality with functional significance in kinase regulation. By reconstructing allosteric communication pathways in the regulatory complexes, we have found that high centrality sites can be directly linked in the interaction networks and form the efficient "information pipeline" for transmitting signals between distant regions.

The implications of these findings may prove useful in predicting drug resistant sites in the SH3 and SH2 domains. Based on this evidence, we are tempted to speculate that binding specificity in the kinase complexes may be partly associated with the emergence of a small number of high betweenness nodes that are allosterically coupled and favor a specific network topology. The removal or weakening of these allosteric links (corresponding to the emergence of drug resistant mutations or changes in the phosphorylation status of key functional residues) may delete long-range bridges leading to a potential network fragmentation. The connection between network properties of kinase structures and differential kinase sensitivities to drug binding suggests that residue interaction networks may be engineered for effective therapeutic intervention targeting specific high centrality nodes. The simplicity and transparency of the network analysis coupled with the rigor of biophysical simulations could provide a useful perspective on structural stability and function, complementing structural and biochemical studies of protein kinase regulation. Integration of computation and experiments within a framework of protein structure networks may inform system-based drug discovery and guide rational design of binding specificities and targeted therapies through understanding of robustness and fragility in complex systems.

ASSOCIATED CONTENT

Supporting Information

The Supporting Information is available free of charge on the ACS Publications website at DOI: 10.1021/acs.jcim.5b00240.

Analysis of functional dynamics and correlated motions in the crystal structures of the catalytic domain of c-Abl and c-Src kinases (Figures SI1 and SI2). Comparison of local and global measures of structural stability in the kinase structures (Figures SI3 and S4). Distributions of residue-based relative solvent accessibility and residue depth (Figures S5 and S6) (PDF)

AUTHOR INFORMATION

Corresponding Author

*Phone: 714-516-4586. Fax: 714-532-6048. E-mail: verkhivk@chapman.edu.

Notes

The authors declare no competing financial interest.

ACKNOWLEDGMENTS

This work was partly supported by institutional funding from Chapman University.

DOI: 10.1021/acs.jcim.5b00240
J. Chem. Inf. Model. 2015, 55, 1645−1662

■ ABBREVIATIONS

SH3, Src homology 3; SH2, Src homology 2; KD, kinase domain

■ REFERENCES

(1) Nolen, B.; Taylor, S.; Ghosh, G. Regulation of Protein Kinases; Controlling Activity Through Activation Segment Conformation. *Mol. Cell* **2004**, *15*, 661−675.

(2) Noble, M. E.; Endicott, J. A.; Johnson, L. N. Protein Kinase Inhibitors: Insights into Drug Design from Structure. *Science* **2004**, *303*, 1800−1805.

(3) Huse, M.; Kuriyan, J. The conformational Plasticity of Protein Kinases. *Cell* **2002**, *109*, 275−282.

(4) Taylor, S. S.; Kornev, A. P. Protein Kinases: Evolution of Dynamic Regulatory Proteins. *Trends Biochem. Sci.* **2011**, *36*, 65−77.

(5) Endicott, J. A.; Noble, M. E.; Johnson, L. N. The Structural Basis for Control of Eukaryotic Protein Kinases. *Annu. Rev. Biochem.* **2012**, *81*, 587−613.

(6) Taylor, S. S.; Keshwani, M. M.; Steichen, J. M.; Kornev, A. P. Evolution of the Eukaryotic Protein Kinases as Dynamic Molecular Switches. *Philos. Trans. R. Soc., B* **2012**, *367*, 2517−2528.

(7) Taylor, S. S.; Ilouz, R.; Zhang, P.; Kornev, A. P. Assembly of Allosteric Macromolecular Switches: Lessons from PKA. *Nat. Rev. Mol. Cell Biol.* **2012**, *13*, 646−658.

(8) Artim, S. C.; Mendrola, J. M.; Lemmon, M. A. Assessing the Range of Kinase Autoinhibition Mechanisms in the Insulin Receptor Family. *Biochem. J.* **2012**, *448*, 213−220.

(9) Oruganty, K.; Kannan, N. Design Principles Underpinning the Regulatory Diversity of Protein Kinases. *Philos. Trans. R. Soc., B* **2012**, *367*, 2529−2539.

(10) Oruganty, K.; Kannan, N. Evolutionary Variation and Adaptation in a Conserved Protein Kinase Allosteric Network: Implications for Inhibitor Design. *Biochim. Biophys. Acta, Proteins Proteomics* **2013**, *1834*, 1322−13229.

(11) Meharena, H. S.; Chang, P.; Keshwani, M. M.; Oruganty, K.; Nene, A. K.; Kannan, N.; Taylor, S. S.; Kornev, A. P. Deciphering the Structural Basis of Eukaryotic Protein Kinase Regulation. *PLoS Biol.* **2013**, *11*, e1001680.

(12) Pluk, H.; Dorey, K.; Superti-Furga, G. Autoinhibition of c-Abl. *Cell* **2002**, *108*, 247−259.

(13) Hantschel, O.; Nagar, B.; Guettler, S.; Kretzschmar, J.; Dorey, K.; Kuriyan, J.; Superti-Furga, G. A Myristoyl/phosphotyrosine Switch Regulates c-Abl. *Cell* **2003**, *112*, 845−857.

(14) Hantschel, O.; Superti-Furga, G. Regulation of the c-Abl and Bcr-Abl Tyrosine Kinases. *Nat. Rev. Mol. Cell Biol.* **2004**, *5*, 33−44.

(15) Boggon, T. J.; Eck, M. J. Structure and Regulation of Src Family Kinases. *Oncogene* **2004**, *23*, 7918−7927.

(16) Roskoski, R., Jr. Src Protein-Tyrosine Kinase Structure and Regulation. *Biochem. Biophys. Res. Commun.* **2004**, *324*, 1155−1164.

(17) Engen, J. R.; Wales, T. E.; Hochrein, J. M.; Meyn, M. A.; Banu Ozkan, S.; Bahar, I.; Smithgall, T. E. Structure and Dynamic Regulation of Src-Family Kinases. *Cell. Mol. Life Sci.* **2008**, *65*, 3058−3073.

(18) Xu, W.; Harrison, S. C.; Eck, M. J. Three-Dimensional Structure of the Tyrosine Kinase c-Src. *Nature* **1997**, *385*, 595−601.

(19) Xu, W.; Doshi, A.; Lei, M.; Eck, M. J.; Harrison, S. C. Crystal Structures of c-Src Reveal Features of Its Autoinhibitory Mechanism. *Mol. Cell* **1999**, *3*, 629−638.

(20) Cowan-Jacob, S. W.; Fendrich, G.; Manley, P. W.; Jahnke, W.; Fabbro, D.; Liebetanz, J.; Meyer, T. The Crystal Structure of a c-Src Complex in an Active Conformation Suggests Possible Steps in c-Src Activation. *Structure* **2005**, *13*, 861−871.

(21) Nagar, B.; Hantschel, O.; Young, M. A.; Scheffzek, K.; Veach, D.; Bornmann, W.; Clarkson, B.; Superti-Furga, G.; Kuriyan, J. Structural Basis for the Autoinhibition of c-Abl Tyrosine Kinase. *Cell* **2003**, *112*, 859−871.

(22) Nagar, B.; Hantschel, O.; Seeliger, M.; Davies, J. M.; Weis, W. I.; Superti-Furga, G.; Kuriyan, J. Organization of the SH3-SH2 Unit in Active and Inactive Forms of the c-Abl Tyrosine Kinase. *Mol. Cell* **2006**, *21*, 787−798.

(23) Smith, K. M.; Yacobi, R.; Van Etten, R. A. Autoinhibition of Bcr-Abl through Its SH3 Domain. *Mol. Cell* **2003**, *12*, 27−37.

(24) Filippakopoulos, P.; Kofler, M.; Hantschel, O.; Gish, G. D.; Grebien, F.; Salah, E.; Neudecker, P.; Kay, L. E.; Turk, B. E.; Superti-Furga, G.; Pawson, T.; Knapp, S. Structural Coupling of SH2-Kinase Domains Links Fes and Abl Substrate Recognition and Kinase Activation. *Cell* **2008**, *134*, 793−803.

(25) Hantschel, O. Structure, Regulation, Signaling, and Targeting of Abl Kinases in Cancer. *Genes Cancer* **2012**, *3*, 436−446.

(26) Panjarian, S.; Iacob, R. E.; Chen, S.; Engen, J. R.; Smithgall, T. E. Structure and Dynamic Regulation of Abl Kinases. *J. Biol. Chem.* **2013**, *288*, 5443−5450.

(27) Reddy, E. P.; Aggarwal, A. K. The Ins and Outs of Bcr-Abl Inhibition. *Genes Cancer* **2012**, *3*, 447−454.

(28) Chen, S.; Brier, S.; Smithgall, T. E.; Engen, J. R. The Abl SH2-Kinase Linker Naturally Adopts a Conformation Competent for SH3 Domain Binding. *Protein Sci.* **2007**, *16*, 572−581.

(29) Hochrein, J. M.; Lerner, E. C.; Schiavone, A. P.; Smithgall, T. E.; Engen, J. R. An Examination of Dynamics Crosstalk between SH2 and SH3 Domains by Hydrogen/Deuterium Exchange and Mass Spectrometry. *Protein Sci.* **2006**, *15*, 65−73.

(30) Panjarian, S.; Iacob, R. E.; Chen, S.; Wales, T. E.; Engen, J. R.; Smithgall, T. E. Enhanced SH3/Linker Interaction Overcomes Abl Kinase Activation by Gatekeeper and Myristic Acid Binding Pocket Mutations and Increases Sensitivity to Small Molecule Inhibitors. *J. Biol. Chem.* **2013**, *288*, 6116−6129.

(31) Chen, S.; Dumitrescu, T. P.; Smithgall, T. E.; Engen, J. R. Abl N-terminal Cap Stabilization of SH3 Domain Dynamics. *Biochemistry* **2008**, *47*, 5795−5803.

(32) Barila, D.; Superti-Furga, G. An intramolecular SH3-Domain Interaction Regulates c-Abl Activity. *Nat. Genet.* **1998**, *18*, 280−282.

(33) Brasher, B. B.; Van Etten, R. A. c-Abl Has High Intrinsic Tyrosine Kinase Activity That Is Stimulated by Mutation of the Src Homology 3 Domain and by Autophosphorylation at Two Distinct Regulatory Tyrosines. *J. Biol. Chem.* **2000**, *275*, 35631−35637.

(34) Brasher, B. B.; Roumiantsev, S.; Van Etten, R. A. Mutational Analysis of the Regulatory Function of the c-Abl Src Homology 3 Domain. *Oncogene* **2001**, *20*, 7744−7752.

(35) Chen, S.; O'Reilly, L. P.; Smithgall, T. E.; Engen, J. R. Tyrosine Phosphorylation in the SH3 Domain Disrupts Negative Regulatory Interactions within the c-Abl Kinase Core. *J. Mol. Biol.* **2008**, *383*, 414−423.

(36) Meyn, M. A.; Wilson, M. B.; Abdi, F. A.; Fahey, N.; Schiavone, A. P.; Wu, J.; Hochrein, J. M.; Engen, J. R.; Smithgall, T. E. Src Family Kinases Phosphorylate the Bcr-Abl SH3-SH2 Region and Modulate Bcr-Abl Transforming Activity. *J. Biol. Chem.* **2006**, *281*, 30907−30916.

(37) Pene-Dumitrescu, T.; Peterson, L. F.; Donato, N. J.; Smithgall, T. E. An Inhibitor-Resistant Mutant of Hck Protects CML Cells Against the Antiproliferative and Apoptotic Effects of the Broad-Spectrum Src Family Kinase Inhibitor A-419259. *Oncogene* **2008**, *27*, 7055−7069.

(38) Schindler, T.; Bornmann, W.; Pellicena, P.; Miller, W. T.; Clarkson, B.; Kuriyan, J. Structural Mechanism for STI-571 Inhibition of Abelson Tyrosine Kinase. *Science* **2000**, *289*, 1938−1942.

(39) Nagar, B.; Bornmann, W. G.; Pellicena, P.; Schindler, T.; Veach, D. R.; Miller, W. T.; Clarkson, B.; Kuriyan, J. Crystal Structures of the Kinase Domain of c-Abl in Complex with the Small Molecule Inhibitors PD173955 and Imatinib (STI-571). *Cancer Res.* **2002**, *62*, 4236−4243.

(40) Levinson, N. M.; Kuchment, O.; Shen, K.; Young, M. A.; Koldobskiy, M.; Karplus, M.; Cole, P. A.; Kuriyan, J. A Src-Like Inactive Conformation in the Abl Tyrosine Kinase Domain. *PLoS Biol.* **2006**, *4*, e144.

(41) Tokarski, J. S.; Newitt, J. A.; Chang, C. Y.; Cheng, J. D.; Wittekind, M.; Kiefer, S. E.; Kish, K.; Lee, F. Y.; Borzillerri, R.; Lombardo, L. J.; Xie, D.; Zhang, Y.; Klei, H. E. The Structure of

DOI: 10.1021/acs.jcim.5b00240
J. Chem. Inf. Model. 2015, 55, 1645−1662

Dasatinib (BMS-354825) Bound to Activated ABL Kinase Domain Elucidates Its Inhibitory Activity against Imatinib-Resistant ABL Mutants. *Cancer Res.* **2006**, *66*, 5790−5797.
(42) Dorey, K.; Engen, J. R.; Kretzschmar, J.; Wilm, M.; Neubauer, G.; Schindler, T.; Superti-Furga, G. Phosphorylation and Structure-Based Functional Studies Reveal a Positive and a Negative Role for the Activation Loop of the c-Abl Tyrosine Kinase. *Oncogene* **2001**, *20*, 8075−8084.
(43) Grebien, F.; Hantschel, O.; Wojcik, J.; Kaupe, I.; Kovacic, B.; Wyrzucki, A. M.; Gish, G. D.; Cerny-Reiterer, S.; Koide, A.; Beug, H.; Pawson, T.; Valent, P.; Koide, S.; Superti-Furga, G. Targeting the SH2-Kinase Interface in Bcr-Abl Inhibits Leukemogenesis. *Cell* **2011**, *147*, 306−319.
(44) Lamontanara, A. J.; Georgeon, S.; Tria, G.; Svergun, D. I.; Hantschel, O. The SH2 domain of Abl kinases Regulates Kinase Autophosphorylation by Controlling Activation Loop Accessibility. *Nat. Commun.* **2014**, *5*, 5470.
(45) Lorenz, S. G.; Deng, P.; Hantschel, O.; Superti-Furga, G.; Kuriyan, J. Crystal Structure of an SH2-kinase Construct of c-Abl and Effect of the SH2 Domain on Kinase Activity. *Biochem. J.* **2015**, *468*, 283−291.
(46) Skora, L.; Mestan, J.; Fabbro, D.; Jahnke, W.; Grzesiek, S. NMR Reveals the Allosteric Opening and Closing of Abelson Tyrosine Kinase by ATP-Site and Myristoyl Pocket Inhibitors. *Proc. Natl. Acad. Sci. U. S. A.* **2013**, *110*, E4437−E4445.
(47) Lamontanara, A. J.; Gencer, E. B.; Kuzyk, O.; Hantschel, O. Mechanisms of Resistance to Bcr-Abl and Other Kinase Inhibitors. *Biochim. Biophys. Acta, Proteins Proteomics* **2013**, *1834*, 1449−1459.
(48) Sherbenou, D. W.; Hantschel, O.; Kaupe, I.; Willis, S.; Bumm, T.; Turaga, L. P.; Lange, T.; Dao, K. H.; Press, R. D.; Druker, B. J.; Superti-Furga, G.; Deininger, M. W. BCR-ABL SH3-SH2 Domain Mutations in Chronic Myeloid Leukemia Patients on Imatinib. *Blood* **2010**, *116*, 3278−3285.
(49) Seeliger, M. A.; Nagar, B.; Frank, F.; Cao, X.; Henderson, M. N.; Kuriyan, J. C-Src Binds to the Cancer Drug Imatinib with an Inactive Abl/c-Kit Conformation and a Distributed Thermodynamic Penalty. *Structure* **2007**, *15*, 299−311.
(50) Seeliger, M. A.; Ranjitkar, P.; Kasap, C.; Shan, Y.; Shaw, D. E.; Shah, N. P.; Kuriyan, J.; Maly, D. J. Equally Potent Inhibition of c-Src and Abl by Compounds That Recognize Inactive Kinase Conformations. *Cancer Res.* **2009**, *69*, 2384−2392.
(51) Aleksandrov, A.; Simonson, T. A Molecular Mechanics Model for Imatinib and Imatinib:Kinase Binding. *J. Comput. Chem.* **2010**, *31*, 1550−1560.
(52) Aleksandrov, A.; Simonson, T. Molecular Dynamics Simulations Show That Conformational Selection Governs the Binding Preferences of Imatinib for Several Tyrosine Kinases. *J. Biol. Chem.* **2010**, *285*, 13807−13815.
(53) Lovera, S.; Sutto, L.; Boubeva, R.; Scapozza, L.; Dölker, N.; Gervasio, F. L. The Different Flexibility of c-Src and c-Abl Kinases Regulates the Accessibility of a Druggable Inactive Conformation. *J. Am. Chem. Soc.* **2012**, *134*, 2496−2499.
(54) Lin, Y. L.; Meng, Y.; Jiang, W.; Roux, B. Explaining Why Gleevec is a Specific and Potent Inhibitor of Abl Kinase. *Proc. Natl. Acad. Sci. U. S. A.* **2013**, *110*, 1664−1669.
(55) Lin, Y. L.; Roux, B. Computational Analysis of the Binding Specificity of Gleevec to Abl, c-Kit, Lck, and c-Src Tyrosine Kinases. *J. Am. Chem. Soc.* **2013**, *135*, 14741−14753.
(56) Lin, Y. L.; Meng, Y.; Huang, L.; Roux, B. Computational Study of Gleevec and G6G Reveals Molecular Determinants of Kinase Inhibitor Selectivity. *J. Am. Chem. Soc.* **2014**, *136*, 14753−14762.
(57) Hari, S. B.; Perera, B. G.; Ranjitkar, P.; Seeliger, M. A.; Maly, D. J. Conformation-selective Inhibitors Reveal Differences in the Activation and Phosphate-binding Loops of the Tyrosine Kinases Abl and Src. *ACS Chem. Biol.* **2013**, *8*, 2734−2743.
(58) Agafonov, R. V.; Wilson, C.; Otten, R.; Buosi, V.; Kern, D. Energetic Dissection of Gleevec's Selectivity Toward Human Tyrosine Kinases. *Nat. Struct. Mol. Biol.* **2014**, *21*, 848−853.
(59) Shan, Y.; Seeliger, M. A.; Eastwood, M. P.; Frank, F.; Xu, H.; Jensen, M.Ø.; Dror, R. O.; Kuriyan, J.; Shaw, D. E. A Conserved Protonation-Dependent Switch Controls Drug Binding in the Abl Kinase. *Proc. Natl. Acad. Sci. U. S. A.* **2009**, *106*, 139−144.
(60) Dixit, A.; Verkhivker, G. M. Hierarchical Modeling of Activation Mechanisms in the ABL and EGFR Kinase Domains: Thermodynamic and Mechanistic Catalysts of Kinase Activation by Cancer Mutations. *PLoS Comput. Biol.* **2009**, *5*, e1000487.
(61) Dixit, A.; Verkhivker, G. M. Computational Modeling of Allosteric Communication Reveals Organizing Principles of Mutation-Induced Signaling in ABL and EGFR Kinases. *PLoS Comput. Biol.* **2011**, *7*, e1002179.
(62) Dölker, N.; Górna, M. W.; Sutto, L.; Torralba, A. S.; Superti-Furga, G.; Gervasio, F. L. The SH2 Domain Regulates c-Abl Kinase Activation by a Cyclin-like Mechanism and Remodulation of the Hinge Motion. *PLoS Comput. Biol.* **2014**, *10*, e1003863.
(63) Corbi-Verge, C.; Marinelli, F.; Zafra-Ruano, A.; Ruiz-Sanz, J.; Luque, I.; Faraldo-Gómez, J. D. Two-State dynamics of the SH3-SH2 Tandem of Abl Kinase and the Allosteric Role of the N-Cap. *Proc. Natl. Acad. Sci. U. S. A.* **2013**, *110*, E3372−E3380.
(64) Tsai, C. J.; Sol, A. D.; Nussinov, R. Protein Allostery, Signal Transmission and Dynamics: A Classification Scheme of Allosteric Mechanisms. *Mol. BioSyst.* **2009**, *5*, 207−216.
(65) Tsai, C. J.; Nussinov, R. The Free Energy Landscape in Translational science: How Can Somatic Mutations Result in Constitutive Oncogenic Activation? *Phys. Chem. Chem. Phys.* **2014**, *16*, 6332−6341.
(66) Vendruscolo, M. N.; Dokholyan, V.; Paci, E.; Karplus, M. Small-World View of the Amino Acids That Play a Key Role in Protein Folding. *Phys. Rev. E: Stat. Phys., Plasmas, Fluids, Relat. Interdiscip. Top.* **2002**, *65*, 061910.
(67) Dokholyan, N. V.; Li, L.; Ding, F.; Shakhnovich, E. I. Topological Determinants of Protein Folding. *Proc. Natl. Acad. Sci. U. S. A.* **2002**, *99*, 8637−8641.
(68) Atilgan, A. R.; Akan, P.; Baysal, C. Small-World Communication of Residues and Significance for Protein Dynamics. *Biophys. J.* **2004**, *86*, 85−91.
(69) Bagler, G.; Sinha, S. Network Properties of Protein Structures. *Phys. A* **2005**, *346*, 27−33.
(70) del Sol, A.; O'Meara, P. Small-World Network Approach to Identify Key Residues in Protein-Protein Interaction. *Proteins: Struct., Funct., Genet.* **2005**, *58*, 672−682.
(71) del Sol, A.; Fujihashi, H.; O'Meara, P. Topology of Small-World Networks of Protein-Protein Complex Structures. *Bioinformatics* **2005**, *21*, 1311−1315.
(72) Sathyapriya, R.; Vijayabaskar, M. S.; Vishveshwara, S. Insights into Protein-DNA Interactions Through Structure Network Analysis. *PLoS Comput. Biol.* **2008**, *4*, e1000170.
(73) Amitai, G.; Shemesh, A.; Sitbon, E.; Shklar, M.; Netanely, D.; Venger, I.; Pietrokovski, S. Network Analysis of Protein Structures Identifies Functional Residues. *J. Mol. Biol.* **2004**, *344*, 1135−1146.
(74) Hu, Z.; Bowen, D.; Southerland, W. M.; del Sol, A.; Pan, Y.; Nussinov, R.; Ma, B. Ligand Binding and Circular Permutation Modify Residue Interaction Network in DHFR. *PLoS Comput. Biol.* **2007**, *3*, e117.
(75) del Sol, A.; Fujihashi, H.; Amoros, D.; Nussinov, R. Residue Centrality, Functionally Important Residues, and Active Site Shape: Analysis of Enzyme and Non-Enzyme Families. *Protein Sci.* **2006**, *15*, 2120−2128.
(76) del Sol, A.; Fujihashi, H.; Amoros, D.; Nussinov, R. Residues Crucial for Maintaining Short Paths in Network Communication Mediate Signaling in Proteins. *Mol. Syst. Biol.* **2006**, *2*, 2006.0019.
(77) Brinda, K. V.; Vishveshwara, S. A Network Representation of Protein Structures: Implications for Protein Stability. *Biophys. J.* **2005**, *89*, 4159−4170.
(78) Vijayabaskar, M. S.; Vishveshwara, S. Interaction Energy Based Protein Structure Networks. *Biophys. J.* **2010**, *99*, 3704−3715.
(79) Ghosh, A.; Vishveshwara, S. A Study of Communication Pathways in Methionyl-tRNA Synthetase by Molecular Dynamics

DOI: 10.1021/acs.jcim.5b00240
J. Chem. Inf. Model. 2015, 55, 1645−1662

Simulations and Structure Network Analysis. *Proc. Natl. Acad. Sci. U. S. A.* **2007**, *104*, 15711−15716.
(80) Ghosh, A.; Vishveshwara, S. Variations in Clique and Community Patterns in Protein Structures During Allosteric Communication: Investigation of Dynamically Equilibrated Structures of Methionyl tRNA Synthetase Complexes. *Biochemistry* **2008**, *47*, 11398−11407.
(81) Bhattacharyya, M.; Vishveshwara, S. Elucidation of the Conformational Free Energy Landscape in H.pylori LuxS and Its Implications to Catalysis. *BMC Struct. Biol.* **2010**, *10*, 27.
(82) Bhattacharyya, M.; Vishveshwara, S. Probing the Allosteric Mechanism in Pyrrolysyl-tRNA Synthetase Using Energy-Weighted Network Formalism. *Biochemistry* **2011**, *50*, 6225−6236.
(83) Sethi, A.; Eargle, J.; Black, A. A.; Luthey-Schulten, Z. Dynamical Networks in tRNA:Protein Complexes. *Proc. Natl. Acad. Sci. U. S. A.* **2009**, *106*, 6620−6625.
(84) Ghosh, A.; Sakaguchi, R.; Liu, C.; Vishveshwara, S.; Hou, Y. M. Allosteric Communication in Cysteinyl tRNA Synthetase: A Network of Direct and Indirect Readout. *J. Biol. Chem.* **2011**, *286*, 37721−37731.
(85) Rivalta, I.; Sultan, M. M.; Lee, N. S.; Manley, G. A.; Loria, J. P.; Batista, V. S. Allosteric Pathways in Imidazole Glycerol Phosphate Synthase. *Proc. Natl. Acad. Sci. U. S. A.* **2012**, *109*, E1428−E1436.
(86) Pfleger, C.; Rathi, P. C.; Klein, D. L.; Radestock, S.; Gohlke, H. Constraint Network Analysis (CNA): A Python Software Package for Efficiently Linking Biomacromolecular Structure, Flexibility, (Thermo-)stability, and Function. *J. Chem. Inf. Model.* **2013**, *53*, 1007−1015.
(87) Krüger, D. M.; Rathi, P. C.; Pfleger, C.; Gohlke, H. CNA Web Server: Rigidity Theory-based Thermal Unfolding Simulations of Proteins for Linking Structure, Flexibility, (Thermo-)stability, and Function. *Nucleic Acids Res.* **2013**, *41*, W340−W348.
(88) Pfleger, C.; Gohlke, H. Efficient and Robust Analysis of Biomacromolecular Flexibility Using Ensembles of Network Topologies Based on Fuzzy Noncovalent Constraints. *Structure* **2013**, *21*, 1725−1734.
(89) Berman, H. M.; Westbrook, J.; Feng, Z.; Gilliland, G.; Bhat, T. N.; Weissig, H.; Shindyalov, I. N.; Bourne, P. E. The Protein Data Bank. *Nucleic Acids Res.* **2000**, *28*, 235−242.
(90) Fernandez-Fuentes, N.; Zhai, J.; Fiser, A. ArchPRED: A Template Based Loop Structure Prediction Server. *Nucleic Acids Res.* **2006**, *34*, W173−W176.
(91) Phillips, J. C.; Braun, R.; Wang, W.; Gumbart, J.; Tajkhorshid, E.; Villa, E.; Chipot, C.; Skeel, R. D.; Kalé, L.; Schulten, K. Scalable Molecular Dynamics with NAMD. *J. Comput. Chem.* **2005**, *26*, 1781−1802.
(92) MacKerell, A. D.; Bashford, D.; Bellott, M.; Dunbrack, R. L.; Evanseck, J. D.; Field, M. J.; Fischer, S.; Gao, J.; Guo, H.; Ha, S.; Joseph-McCarthy, D.; Kuchnir, L.; Kuczera, K.; Lau, F. T. K.; Mattos, C.; Michnick, S.; Ngo, T.; Nguyen, D. T.; Prodhom, B.; Reiher, W. E.; Roux, B.; Schlenkrich, M.; Smith, J. C.; Stote, R.; Straub, J.; Watanabe, M.; Wiórkiewicz-Kuczera, J.; Yin, D.; Karplus, M. All-Atom Empirical Potential for Molecular Modeling and Dynamics Studies of Proteins. *J. Phys. Chem. B* **1998**, *102*, 3586−3616.
(93) James, K. A.; Verkhivker, G. M. Structure-Based network Analysis of Activation Mechanisms in the ErbB Family of Receptor Tyrosine Kinases: The Regulatory Spine Residues are Global Mediators of Structural Stability and Allosteric Interactions. *PLoS One* **2014**, *9*, e113488.
(94) Koukos, P. I.; Glykos, N. M. Grcarma: A Fully Automated Task-Oriented Interface for the Analysis of Molecular Dynamics Trajectories. *J. Comput. Chem.* **2013**, *34*, 2310−2312.
(95) Fraczkiewicz, R.; Braun, W. Exact and Efficient Analytical Calculation of the Accessible Surface Areas and Their Gradients for Macromolecules. *J. Comput. Chem.* **1998**, *19*, 319−333.
(96) Tan, K. P.; Nguyen, T. B.; Patel, S.; Varadarajan, R.; Madhusudhan, M. S. Depth: A Web Server to Compute Depth, Cavity Sizes, Detect Potential Small-Molecule Ligand-Binding Cavities and Predict the pKa of Ionizable Residues in Proteins. *Nucleic Acids Res.* **2013**, *41*, W314−W321.
(97) Floyd, R. W. Algorithm 97: Shortest Path. *Commun. ACM* **1962**, *5*, 345.
(98) Márquez, J. A.; Smith, C. I. E.; Petoukhov, M. V.; Surdo, Lo. P.; Mattsson, P. T.; Knekt, M.; Westlund, A.; Scheffzek, K.; Saraste, M.; Svergun, D. I. Conformation of Full-Length Bruton Tyrosine Kinase (Btk) from Synchrotron X-ray Solution Scattering. *EMBO J.* **2003**, *22*, 4616−4624.
(99) Manley, G.; Rivalta, I.; Loria, J. P. Solution NMR and Computational Methods for Understanding Protein Allostery. *J. Phys. Chem. B* **2013**, *117*, 3063−3073.
(100) Illingworth, C. J.; Scott, P. D.; Parkes, K. E.; Snell, C. R.; Campbell, M. P.; Reynolds, C. A. Connectivity and Binding Site Recognition: Applications Relevant to Drug Design. *J. Comput. Chem.* **2010**, *31*, 2677−2688.
(101) Nagar, B. C-Abl Tyrosine kinase and Inhibition by the Cancer Drug Imatinib (Gleevec/STI-571). *J. Nutr.* **2007**, *137*, 1518S−1523S.
(102) Gonfloni, S.; Weijland, A.; Kretzschmar, J.; Superti-Furga, G. Crosstalk Between the Catalytic and Regulatory Domains Allows Bidirectional Regulation of Src. *Nat. Struct. Biol.* **2000**, *7*, 281−286.
(103) LaFevre-Bernt, M.; Sicheri, F.; Pico, A.; Porter, M.; Kuriyan, J.; Miller, W. T. Intramolecular Regulatory Interactions in the Src Family Kinase Hck Probed by Mutagenesis of A Conserved Tryptophan Residue. *J. Biol. Chem.* **1998**, *273*, 32129−32134.
(104) Gonfloni, S.; Frischknecht, F.; Way, M.; Superti-Furga, G. Leucine 255 of Src Couples Intramolecular Interactions to Inhibition of Catalysis. *Nat. Struct. Biol.* **1999**, *6*, 760−764.
(105) Colizza, V.; Flammini, A.; Serrano, M. A.; Vespignani, A. Detecting Rich-Club Ordering in Complex Networks. *Nat. Phys.* **2006**, *2*, 110−115.
(106) Bagler, G.; Sinha, S. Assortative Mixing in Protein Contact Networks and Protein Folding Kinetics. *Bioinformatics* **2007**, *23*, 1760−1767.

DOI: 10.1021/acs.jcim.5b00240
J. Chem. Inf. Model. 2015, 55, 1645−1662